NTNU – Trondheim
Norwegian University of
Science and Technology

Study on the performance of central solar heating plants with seasonal storage using underground soil in North China and Norway

Hanne Thorshaug Andresen

Master of Energy and Environmental Engineering
Submission date: December 2014
Supervisor: Trygve Magne Eikevik, EPT

Norwegian University of Science and Technology
Department of Energy and Process Engineering

Preface

This report is the written work of my Master thesis at the Norwegian University of Science and Technology (NTNU), Department of Energy and Process Engineering. The subject and later adjustments has been decided in cooperation with Shanghai Jiao Tong University (SJTU) and Norwegian University of Science and Technology (NTNU). The work was done and the thesis written at SJTU, Department of Refrigeration and Cryogenic, during 2014. The title of this master thesis was originally "Study on the performance of central solar heating plants with seasonal storage using underground soil in North China". Due to limitations in the metrological data and discussions with my supervisors the objective has been modified. The title has become " This Study on the performance of central solar heating plants with seasonal storage using underground soil in North China and Mid Norway". The study has been carried out for two different locations Trondheim in Norway and Siping in China.

During my time working on this master thesis I faced certain challenges. The first challenge I came upon was learning the simulation software TRNSYS and understanding how a combined system works. I gain knowledge about the use of transient simulations and the complexity these types of heating systems

Throughout this working period I have received a good guidance and help from my supervisors. I would firstly like to thank my supervisor at SJTU, Professor Yong Li, for his time and feedback on my project this whole time. I also want to thank my supervisor at NTNU, Professor Trygve M. Eikevik for all the support during my work and stay in Shanghai. Last I want to extend my gratitude to all the students working at the Green Energy Laboratory (GEL) for taking time to help me with my work.

I will always be thankful for the experience I have gained by getting this opportunity. Staying in Shanghai has given me countless memories and I have gained academic, social and cultural knowledge that I could not have gained another place.

Shanghai, December 2014

Hanne Thorshaug Andresen

Abstract

This thesis involves the work on a combined system consisting of a solar collector, a geothermal heat pump and borehole ground storage. To fully utilize solar energy this study is based on a heating system deigned to store the solar thermal energy in an underground storage, using U-tube heat exchangers. Renewable energy sources are habitually out of phase with the heating demand, which makes them challenging to fully exploit. Heat from the underground thermal energy storage will be discharged when the solar energy is not sufficient enough, as for the winter months. A simulation model, developed in TRNSYS, is used to simulate the performance of the proposed combined system. The heat load is a single residential building, and the simulation is performed for two different locations. Their difference in design and performance is then analyzed and discussed. The locations used for the system simulations are Trondheim in Norway and Siping in China.

The complexity of a combines system is high due to several options when deciding on the system design. Solar collectors will lift the ground source temperature and in this way reducing the operation time of the heat pump. This will reduce the electricity use in combines systems. The purposes of this study have been to design a combined system for a single house at two different locations, Trondheim **(**63°N, 10°E) and Siping (43°N, 124°E)**.** Studies on the performance of these two systems have then been performed. The focus has been on the thermal energy ground storage, consisting of several boreholes and its temperature behavior. The simulation software TRNSYS was used to analyze the interaction between the different components, the heat losses and gains, the electricity savings and the load requirement. The concept house has been designed in TRNBuild and Meteonorm provides the metrological data used for the different locations. A base case was used as stepping stone for the system optimization; the base case is bases on previous related work.

The system is divided into four different modes simulated separately in TRNSYS. The four simulation modes were solar thermal ground storage, solar direct heating, direct heat exchange with the ground storage and geothermal heat pump. The duration of the modes was divided into the storage season and the heating season.

With the intention to achieve a sufficiently high enough storage end temperature for direct heating of the building when needed, the system design parameters where chosen. The results

of the simulation confirmed that the size and design of the ground storage is of great importance The resulting design for the system located in Trondheim consists of 11boreholes spaced 1.5m apart. However for Siping the optimal design consists of 4 boreholes with a pacing of 2.5m. Both systems has ground storage volume of 623.24m^3 at 30m depth, a solar collector of 200m^2 and a water tank with a volume of 10m^2. With these parameters the storage end temperature was above 40^oC for both and compliable for heating. The heating season was found to be from September to March for Trondheim and from October to May for Siping.

Simulations of the solar direct heating mode show that this mode can cover 19.2% of the heating load for the system located in Trondheim and as much as 47.5% for the system in Siping. The direct heat exchange with the ground covers 27.9% of the heating load in Trondheim, only 11.97% of the heating load is covered by this mode for Siping. The geothermal heat pump covers the largest part of the heating load in Trondheim with 52.9%, while it covers 40.53% of the heating demand in Siping. The initial depth of 30m resulted in freezing boreholes for both location and consequently the depth was changed to 150m for Trondheim and 200m for Siping. The COP was found to be 2.78 and 2.54 for Trondheim and Siping respectfully.

Sammendrag

Denne oppgaven inneholder resultater fra arbeidet med et kombinert system bestående av en solfanger, geotermisk varmepumpe og lagring i borehull. For å kunne utnytte energien fra solen er dette studie basert på et varmesystem designet for å lagre termisk solenergi under joden. Fornybare energikilder er ofte ute av fase i forhold til det gjeldene oppvarmingsbehovet, noe som gjør dem vanskelig å utnytte til det fulle. Varmen som lagres borehullene hentes i den perioden av året hvor den termiske solenergien ikke er tilstrekkelig nok. En simuleringsmodell utviklet i simuleringsprogrammet TRNSYS blir brukt til å simulere systemets ytelse. Varmebelastningen er en typisk familie bolig, og simuleringen er utført for to steder. Påvirkninger fra ytre faktorer har blitt undersøkt og hvordan dette virer inn på systemets design og resultat. Simuleringen er gjort for Trondheim i Norge og Siping i Kina.

Kompleksiteten i en kombinerer systemet er høy grunnet flere mulige design alternativer. Solfangere kan redusere elektrisiteten som brukes i et kombinerte systemer ved å løfte grunntemperaturen og derav redusere driftstiden for varmepumpen. Hensikten med dette studie har vært å designe et kombinert system for en enebolig lokalisert to forskjellige steder, og studere resultatene for systemene. Simuleringsprogrammet TRNSYS har blitt brukt til å analysere samspillet mellom de ulike komponentene, varme tap og utbytte, strømbesparelser og boligens varme kravet. Test boligen har blitt designet i TRNBuild og den metrologiske data er gitt av Meteonorm. En ”base case” ble brukt som springbrett for systemet optimalisering; base case er baser på tidligere relatert arbeid.

Systemet er delt inn i fire forskjellige deler, hver del er simulert separat i TRNSYS. De fire simulerings modellene er lagring av solvarme underjorden, direkte bruk av solvarme til oppvarming, direkte varmeveksling med borehullene og geotermisk varmepumpe. Varigheten av de ulike delene ble delt inn i lagringssesong og fyringssesongen.

Det er lagt fokus på å oppnå høy nok slutt temperatur i borehullene etter endt lagringssesong for direkte oppvarming av bygningen når det er nødvendig. Resultatene av simuleringen bekreftet at størrelsen og utformingen av undergrunns lageret er av stor betydning For systemet lokalisert i Trondheim ble det resultatet et lager bestående av 11 borehull plassert 1.5 m fra hverandre. For Siping er det optimale design bestående av 4 borehull med en

avstand på 2.5 m. Begge systemene har et lagringsvolum på 623.24m^3 , en dybde på 30m, en solfanger på 200m^2 og en tank med et volum på 10m^3. Slutt temperaturen i borehullene er ved disse dimensjonene over 40°C for begge og kompatibel for oppvarming. Fyringssesongen ble funnet å være fra september til mars for Trondheim og fra oktober til mai for Siping.

Simuleringer av modellen for direkte bruk av solvarme **til** viser at 19.2% av varmebelastningen kan dekkes for systemet i Trondheim og så mye som 47.5% for systemet i Siping. Den direkte varmeveksling med borehullene dekker 27.9% av varmebehovet i Trondheim, mens bare 11.97% av det totale for Siping dekkes av denne modellen. Den geotermisk varmepumpen dekker den største delen av varmebelastningen i Trondheim med hele 52.9%, mens den dekker 40.53% av oppvarmingsbehovet i Siping. Den opprinnelige dybde på 30m resulterte i jordtemperaturene under 0^oC og frossen borehull for begge områdene. Borehull dybden ble derfor endret til 150m for Trondheim og 200m for Siping. Trondheim og Siping har hver en COP på 2.78 og 2.54.

Table of Contents

Nomenclature 5
Symbol list 5
Abbreviations 5
Subscripts 6

1. Introduction 7

2. Theory 9
2.1. Background 9
2.2. Energy consumptions in buildings 11
2.3. Seasonal Thermal Energy Storage 11
2.4. Underground thermal energy storages 12
2.5. Borehole Thermal Energy Storage 14
2.6. Geological formation 14
2.7. Balance of thermal loads 17

3. Overview of the proposes heating system 18
3.1. Working principles of the operation modes 18
3.1.1. Mode 1: Solar ground thermal storage 19
3.1.2. Mode 2: Solar direct heating 20
3.1.3. Mode 3: Direct heat exchange with boreholes 20
3.1.4. Geothermal heat pump 21
3.2. Geothermal heat pump 21
3.2.1. Vertical closed loop system 22
3.2.2. Horizontal closed loop pump 22
3.2.3. Working principles 23
3.2.4. COP – predicting the performance 24
3.3. Solar collector 24
3.3.1. General construction of a solar collector 25
3.3.2. Evacuated tube solar collector 26
3.3.3. Collector efficiency and solar fraction 27
3.4. Stratified water tank 27

4. Description of the TRNSYS Software 29
4.1. TRNSYS 29
4.2. Introduction to the concept house and location 29
4.2.1. TRNBuild 29
4.2.2. Heat flows 30
4.3. Building layout and properties 30
4.4. Weather Conditions 31
4.4.1. Weather conditions and demography for Norway 32
4.4.2. Weather conditions and demography for China 32

5. Base Case Parameter 34

6. Simulation and results 36
6.1. Temperature and radiation 36
6.2. Simulation of the concept house 39
6.3. Simulation of Operation mode 1: The solar thermal ground storage mode 42
6.3.1. Investigating the behavior of the Solar Collector and efficiencies 43
6.3.2. Sizing the Solar Collector area 48
6.3.3. Designing the ground storage 53
6.3.4. Optimization of number of boreholes and spacing 60

6.3.5. Tank volume 64
6.4. Simulation results of designing the solar ground storage model 66
6.4.1. Sizing the ground storage and the solar collector 66
6.4.2. The affect of the storage temperature and heat capacity 67
6.4.3. Designing the BTES 68
6.5. Storage mode – simulation of the operation condition 68
6.6. Simulation and results of operation mode 1 72
6.7. Simulation of the different heating modes 75
6.8. Simulation of operation mode 2 76
6.9. Simulation of operation mode 3 83
6.10. Simulation of operation mode 4 86
6.11. Results 91
7. Conclusion **95**
8. Further improvement **97**
Appendix A. Concept House **101**
Appendix B. Component Description **103**
Appendix C. Tables and Results for storage mode Trondheim, Norway **105**
Appendix D. Tables and Results for storage mode Siping, China **107**
Appendix E. Tables and Results the storage mode **108**
Appendix F. Tables and Results the heating modes **109**
***G.1.* Mode 2: Solar direct heating mode 109**
Appendix G. Calculations 110
***G.2.* Calculations of Building heat load 110**
***G.3.* Ratios and efficiencies 110**
***G.4.* Calculations of the efficiencies in the solar collector, Trondheim 112**
***G.5.* Calculations of the COP, Trondheim 113**
***G.6.* Calculations of heat per tube length 113**
***G.7.* Calculations of the new storage parameters for heating mode 4 ..... 114**

List of figures

Figure 1:Borehole thermal energy storage built in Crailsheim, 2007[11] 10
Figure 2: Seasonal storage proposed by Chapuis and Bernier, 2009[12] 11
Figure 3: Different underground thermal energy storages 13
Figure 4: Illustration of energy storage 15
Figure 5:Heat flows in borehole thermal energy storage 16
Figure 6: Horizontal closed loop system
Figure 7: Vertical closed loop system 23
Figure 8: Water circulation through a heat pump, 1. Condenser, 2. Expansion valve, 3. Evaporator 24
Figure 9:Principal sketch of a solar collector 25
Figure 10: Sketch of an evacuated tube solar collector 26
Figure 11: Monthly average temperature Trondheim, Norway 36
Figure 12:Monthly average temperature Siping, China 37
Figure 13: Monthly average solar radiation on horizontal plate Trondheim, Norway 38
Figure 14: Monthly average solar radiation on horizontal plate Siping, China 38

Figure 15: Heat load characteristics for the concept house located in Trondheim, Norway over a year 40
Figure 16: Heat load characteristics for the concept house located in Siping, China, over a year 40
Figure 17: Simplified TRNSYS screenshot of operation mode 1, Solar thermal ground storage 42
Figure 18: Illustration of the solar collector gain and losses 43
Figure 19: Storage temperature over the entire storage season with varying solar collector area in Trondheim, Norway 49
Figure 20: Storage temperature over the entire storage season with varying solar collector area in Siping, China 49
Figure 21: Stored Energy and useful energy with varying solar collector area, Trondheim
Figure 22: Stored Energy and useful energy with varying solar collector area, Siping 50
Figure 23: Storage Temperature with varied depth over the storage season 55
Figure 24: Storage end temperature for different borehole depths in Siping, China 55
Figure 25: Energy loss and gain for different borehole depth in Trondheim. 57
Figure 26: Energy loss and gain for different borehole depth in Siping. 58
Figure 27: Storage losses for different borehole depth in Trondheim, Norway 59
Figure 28: Storage losses for different borehole depth in Siping, China 59
Figure 29: Optimizing the boreholes spacing, energy flows in the ground storage during storage season for Trondheim. 61
Figure 30: Optimizing the boreholes spacing, energy flows in the ground storage during storage season for Siping 62
Figure 31: Borehole design for the Base Case, Trondheim and Siping. 63
Figure 32: Storage temperature with different boreholes spacing during the storage season for Trondheim. 63
Figure 33: Storage temperature with different boreholes spacing during the storage season for Siping. 64
Figure 34: Storage temperature, energy gains and losses during the storage season with different tank volume, Trondheim 65
Figure 35: Heat loss and gains for different storage periods, Trondheim 69
Figure 36: September as starting month 70
Figure 37: August the starting month 70
Figure 38: Energy gains and losses during the storage season for Trondheim and Siping during a typical year 74
Figure 39: Simplified TRNSYS Sketch of operation mode 2, Solar direct heating 77
Figure 40: Simulation of Mode 2 over the entire heating season, Trondheim. 79
Figure 41: Simulation of Mode 2 over the entire heating season, Siping 79
Figure 42: Energy supplied by the heating coil and the heating demand during the entire heating season, Trondheim 80
Figure 43: Energy supplied by the heating coil from the solar collector and the heating demand during the entire heating season, Siping. 81
Figure 44: Solar radiation and solar fraction during the entire heating season, Trondheim. 82
Figure 45: Solar radiation and solar fraction during the entire heating season, Siping. 82
Figure 46: Simplified TRNSYS sketch of operation mode 3, direct het exchange with the ground 83
Figure 47: Temperature distribution during the entire heating season for direct heat exchange with the ground, Trondheim. 85

Figure 48: Temperature distribution during the entire heating season for direct heat exchange with the ground, Siping 85
Figure 49: Simplified TRNSYS sketch of operation mode 4, geothermal heat pump 86
Figure 50: Temperatures during the entire heating season with a storage depth of 30m, Trondheim
Figure 51: Temperatures during the entire heating season with a storage depth of 30m, Siping.
Figure 52: Temperatures during the entire heating season with a storage depth of 150m, Trondheim.
Figure 53: Temperatures during the entire heating season with a storage depth of 200m, Siping. 89
Figure 53: Amount of heat supplied in the different modes use in the heating modes for Trondheim and Siping. 92
Figure 55: Amount of electricity used for the different heating modes for Trondheim and Siping 93

List of tables

Table 1:Building Parameters 31
Table 2: The buildings major characteristics 31
Table 3:Parameters base case 34
Table 4: Overview of the power demand for the space heating of the concept house for Trondheim and Siping 41
Table 5: Heating and cooling seasons 41
Table 6: Operation scheme for heating mode 2 43
Table 7: Efficiencies and rates with varied collector area 47
Table 8: Initially properties for the BTES 53
Table 9: Borehole depth and storage volume, number of boreholes and spacing kept constant. 54
Table 10: Ratio between the collector area and the boreholes volume 54
Table 11:Varied depth and storage end temperature 56
Table 12: Borehole spacing and number of boreholes 60
Table 13: Design parameters for the ground storage for Trondheim and Siping 62
Table 14: COP for the ground storage 71
Table 15: Design parameters for Trondheim and Siping after simulation of operation mode 1. 72
Table 16: Storage temperature after the storage season 74
Table 17: COP for the storage season for both locations, calculated from Equation 15. 74
Table 18: Operation scheme heating mode 3 77
Table 19: Operation scheme heating mode 3 83
Table 20: Operation scheme heating mode 4 86
Table 21: Heat supplied in the different modes use within the heating system 91
Table 20: Results for operation of the different modes 94

Nomenclature

Symbol list

A	area (m^2)
C	total amount of energy (kJ)
E	specific heat capacity (kJ/kgK)
F	fraction (-)
H	enthalpy (kJ/kg)
I	solar radiation per square meter solar collector (kJ/hrm2)
m	mass flow rate (kg/s)
Q	energy rate (kJ/h)
SF	solar fraction (-)
T	temperature (°C)
ΔT	temperature difference (°C)
V	volume (m3)
W	electrical energy consumption (kJ)
η	thermal efficiency of the solar collector

Abbreviations

ATES	Aquifer Thermal Energy Storage
BTES	Borehole Thermal Energy Storage
BES	Borehole Energy Storage
COP	Coefficient of Performance
GSHP	Ground Source Heat Pump
GEL	Green Energy Lab
HP	Heat Pump
HWT	Hot Water Tank
SC	Solar Collector
STES	Solar Thermal Energy System
TRNSTS	Transient System Simulation Program
UTES	Underground Thermal Energy Storage

Subscripts

airbypass	air bypassing the heating coil
building	Concept house (heat load)
out	outlet/exiting
in	inlet/entering
s	solar

1. Introduction

The focus on renewable energy sources for space and water heating has increased in later time. To maintain today's standard of living, the energy consumption cannot be avoided but need to be used more efficiently and with a larger share of renewable resources [1]. This makes seasonal energy storage a viable solution of great value. The majority of the currently heating systems are not environmentally friendly, and substitutes to the traditional heating systems are required to face the hurdle of harmful emissions.

Solar energy is an unlimited renewable energy source, with great potential. Radiation from the sun strikes all over the world and is an important source for space heating applications. It is not the amount of solar radiation that is a barrier for its use but the fact that the availability and demand often is out of phase [2]. The seasonal mismatch between high solar irradiation in the summer and high heat demand in the winter can be balances by seasonal heat storage [3]. The heating and cooling load for an office building is uncertain since it is dependent on the number occupants and duration of occupancy. This makes it difficult to design an exact solar system to complement the mismatch between heating load and cooling load for buildings [4]. This paper presents a GTHP in combination with solar thermal energy and BTES for heating of a residential building. The system study will be done using TRNSYS simulations.

The worlds total energy consumption is distributed over different sectors. There are ways to reduce the energy consumptions in buildings one example is better insulations. It is equally important to look at which energy sources that supply the energy to cover the energy demand in buildings. By implementing renewable sources of energy like solar energy, wind energy and at the same time reduce the use of coal, one will reduce the emissions.

In Europe the construction of new buildings are not high. This indicates that the key for energy reductions lies in enhancing the existing buildings. By focusing on implementing renewable energy sources and adding insulations and other energy reducing materials, older buildings can become energy efficient as well. India and China experiences a rapidly increasing in population and accounts for the main share of the new constructions worldwide. It is therefore important that new buildings and other contractions are builds with energy usage and emission outlet in mind.

In Norway the building sector consist of 2, 2 million units. These households stand for a great amount of the energy sector with yearly stationary energy consumption on 45 TWh, which corresponds to 27 percent of the total stationary energy consumption [5]. Of these 35 TWh are supplies by electricity. The energy consumption in households depends on several factors; number of households, number of household members, temperature, living space and household finances. Heating of the building, water heating, lights and operation of household equipment is accountable for the energy demands in most houses [5].

Energy efficiency in the buildings sector is an important step for the reinforcement of supply, and will help the greenhouse gas emissions. Through national climate agreements the politicians have recognized this as necessarily. Private property owners are the key decision makers since as much as 90% of all houses in Norway are private homes [6]. When we talk about the housing sector it is favorable to divide the sector into two groups: existing homes and new homes. When we look at the energy performance, the degree of energy efficiency, new houses are for filling most of the demands.

China's building stock is characterized by new construction and a focus on speeding up the building mass instead of improving existing buildings [8]. The rapid increase in new constructions to keep up with the urban expansion results in large challenges regarding climatic conditions. In the north part of China where the temperature reaches far down the residents are mostly heated with district heating [8]. Considerably energy saving can be achieved if there is a larger encouragement for conservation and smart solutions. China is a large country that experienced both cold and hot weather, the need for heating and cooling are present and electrical ventilation is commonly used. Balancing the need for new construction as well as the preservation of existing space heating/cooling solutions are challenging.

The aim is to reduce the energy consumption in buildings and produce energy from renewable energy sourced. By having diversity in the source for the energy the supply will be more reliable and environmentally beneficial.

2. Theory

In these section different prior projects relevant to this thesis is presented. The section also contains explanations of seasonal thermal energy storage, underground thermal energy storage, borehole thermal energy storage. It discusses the geological formations and the balance of thermal loads.

2.1. Background

Bauer et al[9]introduced a pilot borehole thermal energy storage in Germany in 1997. It was the first central solar heating plant with borehole thermal energy storage. The BTES contained a volume of 63360m^3 with 528 boreholes at a depth of 30m, and the system would deliver heat for 300 apartments. Solar collectors were installed on different buildings. If neither the tank nor the BTES are able to cover the heating demand a gas-condensing boiler will be used. This system did not reach a wanted solar fraction of 50% and the return temperatures were measured to be higher tank expected, around 47-50^oC.

In 2007 a borehole thermal energy storage build in Crailsheim revealed the rapid growth within this technology. A total of 88 boreholes placed at a depth of 55m comprising a volume of 37500 m^3 [10]. A storage buffer tank of 480m^3 was need due to high capacity rated of the solar collector in the summer. The buffer storage tank charges the heat to the BTES over a longer period of time. A diurnal storage tank of 100m^3 transfers the heat from the seasonal storage either directly or via a heat pump. The storage capacity is increased due to the heat pump in addition to higher usability. The temperature level in the BTES is reduced resulting in decreases storage heat losses. It was shown that the efficiency of the CSHPSS is more robust against high return temperatures.

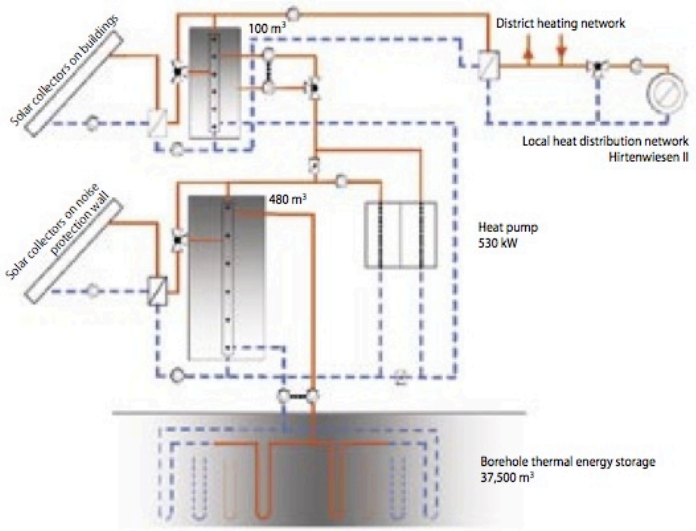

Figure 1:Borehole thermal energy storage built in Crailsheim, 2007[11]

In 2002 a partly solar heated residential area were build in Anneberg, Sweden [11]. The residential area consisted of 50 units with an annual heat demand of 550 MWH. The heat distribution system consists of solar collectors connected and DHW buffer storage. For supplementary heating electric back-up heaters are used. The system performance was tested an evaluated by the simulation software TRNSYS, MINSUN and the DST ground storage module. The system in Anneberg is a low temperature heating system. It was designed for a supply/return water temperature of 32^{o}C/27^{o}C. The annual storage temperature was found to be 30-45^{o}C. The collector operation temperature is flow 40^{o}C and return 60^{o}C. The solar fraction of the system was found to be of 70% after 3-5 years of operation [11].

Results from a seasonal storage proposed by Chapius, S and M. Bernier, show that it is possible to keep the annual seasonal storage temperature slightly above the annual mean ambient temperature [12]. To achieve this results there should be used a solar collector with a small collector area to give high solar collector efficiency. This will reduce the heat losses and raise the solar collector efficiency; the storage temperature will be kept low. To cover the space heating demand a heat pump is used to raise the temperature level. The DST model is used during the simulations performed in TRNSYS. By combining the heat pump results show that the system reaches a solar fraction of 78%[12].

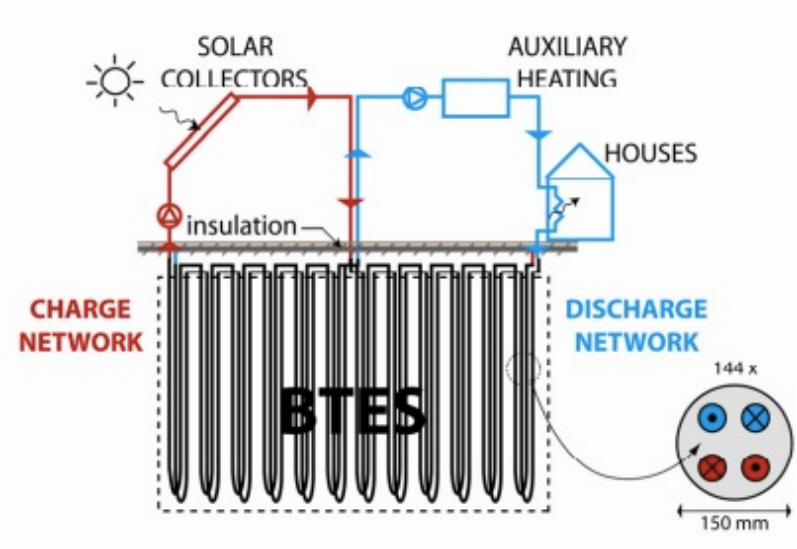

Figure 2: Seasonal storage proposed by Chapuis and Bernier, 2009[12]

2.2. Energy consumptions in buildings

The household energy consumption is affected and influenced by several factors. A household consists of the building type, the building size, the occupants and where the resident is located.

The outdoors temperature at a given location abundantly influences the household energy consumption for a resident. Space heating and hot water demand varied with the diurnal cycle. As the temperature drops during the winter months the heating demand in buildings rises and decreases again when the temperature rises towards the summer, the heat requirement is varying accordingly to the outdoor temperature [7].

2.3. Seasonal Thermal Energy Storage

Thermal energy storage is a way to store thermal energy temporary. The duration can be hours, days or up to several months [13]. Thermal energy storage is therefore divided into long term/seasonal and short term based on the storage duration [13]. The energy storage is either at low or high temperatures, and with several available technologies thermal energy storage satisfies a lot of needs. It is a powerful instrument to secure the delivery of clean energy in a smart energy system. The stored energy can be used in different scale like houses, towns or regions making it highly applicable.

Thermal storage systems can either be passive or active. The active storage concept is chosen here and can be divided into two main sub-systems. These two differ in the way the storage medium circulates within the system. The first sub-system is a direct system that is used in this thesis, this system is also known as a closed loop system. Here the heat storage medium also circulates in the solar collectors. The second sub-system is the indirect system, which is an open loop. In an indirect system different medium are used to collect and store heat [14].

Thermal energy storage is the key to make solar thermal technology fully equipped for space heating and domestic hot water production. As previously mentioned there is often a mismatch between energy supply and demand since solar energy is dependent of weather conditions and the time of day. Seasonal storages are therefore important to ensure reliable delivery of energy, making solar thermal technology economical competitive and environmentally beneficial. Seasonal thermal energy storage primarily stores energy in the summer so it can be discharged for space heating in the winter.

By using thermal energy storage we can reduce the CO_2 emission, lower the need of costly peak and heat production. It will be possible to replace heat and cold production from fossil fuels [15]. There are some challenges when it comes to this type of storage technology. The economical side is a major issue and the stability of storage performance related to material properties ought to be improved. Seasonal storage has as mentioned a great potential in practical applications, but is technological challenging. It requires large storage volumes and is then exposed to greater risks of heat losses.

2.4. Underground thermal energy storages

The most promising technologies for seasonal storage are found underground. The UTES can be used both as an energy sink and energy source. This is dependent on how the demand and supply behaves relatively to each other. Thermal can handle the mismatch supply and demand, as well as the solar fluctuation in solar heating systems.

UTES will always experience energy losses as a function of time. The storage time, storage temperature, storage volume, storage geometry and thermal properties of the storage medium are properties affecting the losses. There are mainly four typed of UTES: water tank, water gravel pit, aquifer thermal energy storage and borehole thermal energy storage. The type

chosen are selected based on the geological and hydrogeological situation in the ground at the relevant location [9].

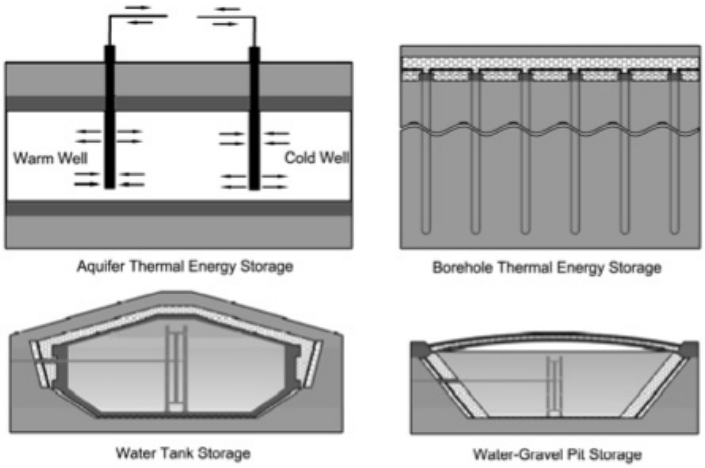

Figure 3: Different underground thermal energy storages

A water tank can be build almost regardless of geological formation. The tank is created by reinforced concrete and can be partially buried or fully buried in the ground [16]. To obtain the heat the tanks walls are thermally insulated.

In gravel-pit storage the heat is charged into and discharged out of the store either by direct water exchange or by plastic piping installed in different layers inside the storage [16]. The gravel-pit storage is insulated at the sidewalls and must be waterproofed as it is buried into the ground. The volume needed for gravel-pit storage is higher than for a water tank. The reason for this is that the gravel-water mixture that has a lower specific heat capacity than water alone.

Aquifers are layers below ground with high hydraulic conductivity [16]. The layer can be filled with distributed sand, limestone, gravel or sandstone. The storage have wells drilled inn for extraction or injection of groundwater in the aquifers. Cold groundwater is extracted from the cold well when the storage is charging. During discharge the flow direction is reversed. The ground properties and geological formation have affects the aquifer storage greatly and need to be investigated beforehand.

2.5. Borehole Thermal Energy Storage

In BTES there will be heat transfer between the heat carrier fluid and the storage. The heat transfer will happen in the U-tube heat exchanger. The U-tubes have a 180 degrees bend at the end and the heat is stored directly in the ground. The boreholes are stored below ground in a distance from around 10-200 meter. The heat transfer from the duct system to the surroundings is driven by heat conduction. The temperature will decrease from the center and towards the boundaries due to the heat losses to the surroundings.

The temperature distribution in BTES is decreasing with time due to heat losses to the surrounding grout and ground region. If we consider the injected heat as a constant heat source over the measuring time period, the temperature in the tube will rise until the there is equilibrium between the ground and pipe. There will also be used layers of insulation around the pipe to decrease the heat losses and conserve the injected heat.

BTES is used in the proposed heating system to store solar thermal excess heat in periods where the demand is low but the energy source is present. In the periods with a het demand the borehole will function as a heat source for the heat pump. When heat is extracted from the ground storage to cover the heating demand the storage temperature will have a decreasing tendency. Heat pumps in combination with thermal energy storage experience a higher efficiency and coefficient of performance.

2.6. Geological formation

An energy system relies on an optimal design fitting its purpose. Borehole thermal energy storage has the purpose of covering the growing need for conservation of energy. A GSHP can practically be installed at any location, but the geothermal parts rely on suitable geological conditions [17]. Local geological conditions are important when designing the system in a matter that provides a successful and sustainable design. Geological and hydrological situation of a site need to be investigated so the ground related parameters could be presented [18]. The ground properties are of great importance when it's important to know how the temperature varies with time and depth from the surface.

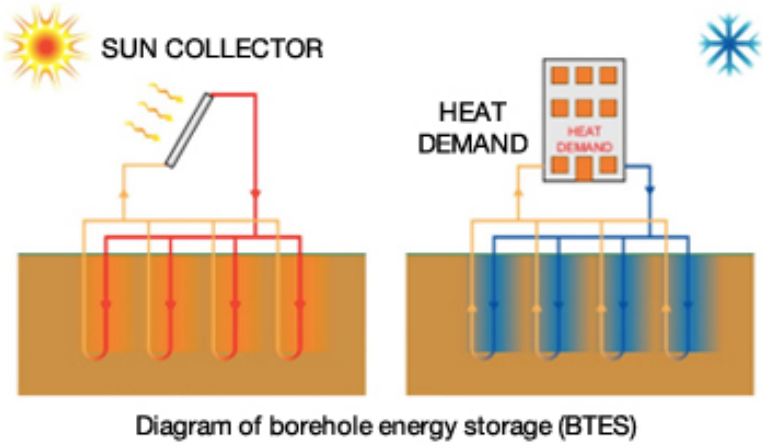

Figure 4: Illustration of energy storage

A vertical closed loop system can have depths varying from one meter to several hundred meters. The system can be configured to supply one single dwelling or large buildings.

The earth temperature will naturally change due to several factors. For a depth beyond 1 meter the earth temperature is closely linked to the seasonal and diurnal cycles, like the air temperature, precipitation and solar radiation. When the depth extends to 9-12 meter the annual fluctuation still makes the earth temperature varying [18]. When reaching a certain depth the temperature is kept content at a certain level unaffected by the metrological changes throughout the year. This is applicable for depths around 15 meters. The constant temperature at these depths is approximately equal the mean annual temperature [17]. When the depth is more than 15 meter the geothermal gradient affects the temperature. The earth natural heat flow keeps increases the temperature with increasing depths. From this we can divide the temperature distribution into three categories:

1. Surface zone: down to 1 meter
2. Shallow zone: 1-8 meter (dry soil) and 20 meter (moist soil) influenced by seasonal variations but are mostly kept constant.
3. Deep zone: below 8-20 meter, ground temperature is constant, increasing with depth according to the geothermal gradient.

By studying the ground properties at the chosen location the GSHP can be designed to result in a minimum temperature difference between the fluid in a given heat exchanger and the

undisturbed ground temperature. An optimal ground will result in a design where the heat exchanger will cover the amount of injected/extracted heat required from the building load within the EWT limits (temperature of the fluid entering the heat pump). This will result in size optimizations and cost reduction. Ground factors that affects the system design is:

- Surface temperature
- Subsurface temperature (down to 10-200m)
- Thermal conductivities and diffusivity of the soil and rock layers
- Groundwater levels and flows
- Aquifer propertied (open loop)
- Rock strength (when considering drilling)

The groundwater has an impact on both a closed and open system. Thermal properties are diminished when rocks become unsaturated and hence the groundwater levels impact the heat exchangers performance. Groundwater flow will transport heat and affects the heating and cooling performance for both an open and closed system Downward and upward groundwater.

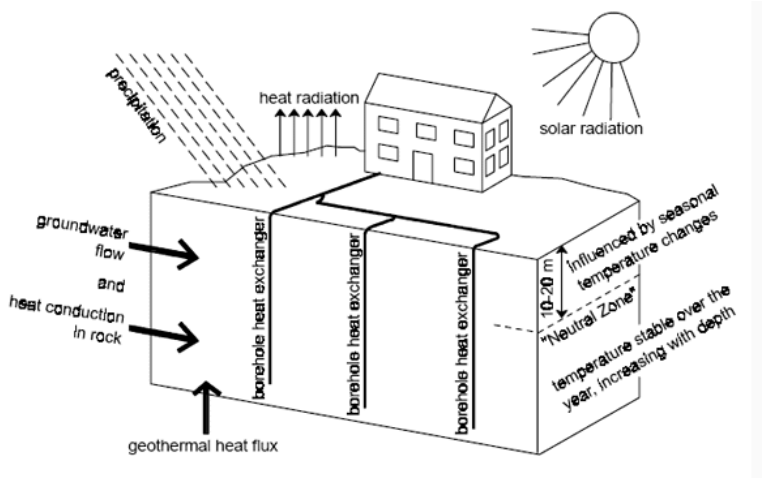

Figure 5:Heat flows in borehole thermal energy storage

The rate of witch heat can be transferred to the heat exchanger from the ground or to the heat exchanger from the ground, or to the ground is determined by the thermal properties of the ground

2.7. Balance of thermal loads

The ground temperature will stabilize at a certain depth, discussed in the previous section. To achieve a good performance and consequently high storage temperature the balance of the thermal are important. The amount of heat extracted compared to the amount that is injected should be equivalent, or as equal as possible. During the duration of operation heat will be extracted in the winter and the heat injected in the summer should compensate for this amount. During the winter and summer time the ground temperature changes are small and the performance of the system can be kept high if we have a good balance. If the amount of heat extracted is higher than the amount injected the storage temperature will gradually decrease resulting in a lower degree of performance. The temperature of the earth is higher than the surroundings but cannot supply enough heat to cover the heating demand over a long time span. In the transient period the temperature reduction can be recovered by enlarging the storage size to moderate the effect. An increase in storage size can be very costly and this need to be evaluated as a govern factor. Introducing a solar collector that can charge the boreholes during the summer can increase the storage temperature. The solar collector will help increase the pumps operations conditions during winter.

Different factors and uncertainties make it difficult to design system with precise stability. The amount of energy extracted and injected in the ground relies on a lot of factors hard to establish. These may be the establishing the correct building load since it is difficult to know the behavior of the occupants, the weather conditions at the given sight affects the ground storage and load.

3. Overview of the proposes heating system

In the following section the proposed heating system is presented. There are four operation modes in this system and they are all described here. The working principle of the operation modes is presented. Further more the major components utilized are presented. This encloses the geothermal heat pump, the solar collector and the stratified water tank.

3.1. Working principles of the operation modes

The proposed heating system that is simulated combines a solar collecting system with BTES and a ground couplet heat exchanger. A water tank connects the solar collector and the ground storage. The simulation accounts for the indoor air-conditioning system and the heat sources present in the system are the solar thermal energy and the ground storage thermal energy. To switch between these modes several valves are used. All the working fluid in the system is water, and can flow through the SC, the HWT, the BTES and the heat distribution system.

The system is divided into four different operation modes; solar thermal ground storage, solar direct heating, direct heat exchanger and geothermal heat pump. The first mode is in operation during the storage season while the remaining is in operation during the heating season. The modes are investigated separately and presented in prioritized order. The operation modes are portrayed in section 7.1.

Operation modes:
Operation mode 1: Solar thermal ground storage
Operation mode 2: Solar direct heating
Operation mode 3: Direct heat exchange with the ground storage
Operation mode 4: Geothermal heat pump

The first mode is the solar thermal ground storage mode, which takes effect through the whole storage season. This is the only storage mode, the three following modes all are in operation during the heating season. Solar thermal energy collected by the solar collectors is transferred to the water tank. The water in the tank exchanges heat to the heat carrier fluid, which circulates through the boreholes. The whole ground temperature has an increasing tendency and the thermal energy is injected to the ground through the interaction between the boreholes and the ground. An on/off differential controller controls the solar collector.

In the solar direct heating mode, which is the second mode, the solar collector is used to produce heat during the heating season. The system delivers hot water directly to the fan coil-heating terminal if the water temperature in the tank is hot enough for space heating (30°C-35°C). A solar water storage tank is used to exchange heat with the passing air that is passing through the fan coil unit.

The third mode is the direct heat exchanger mode. This mode takes effect when the solar collector cannot provide sufficient temperature for use in the heating system. The boreholes are used to produce heating by direct heat exchange in this mode. The heat injected into the ground during storage season is extracted by the ground heat exchanger to cover the space heating demand. The ground temperature should be higher than 30°C for this mode to be in operation. The ground temperature keeps a decreasing tendency since heat is extracted from the storage. This mode should be used before the geothermal heat pump.

The geothermal heat pump mode is the fourth and last mode. This mode set in use when the ground temperature drops to a certain level. Then the heat cannot be utilized to direct heat exchange. The heat pump is then set in operation and reduces its power by extracting the remaining heat from the ground storage. The decreasing temperature tendency continues but the ground storage is used as a heat source for the geothermal heat pump. Due to the heat from the storage the compressor needs less work input and the COP will be high. The source temperature will be around 20°C-30°C.

The ground storage mode is referred to as base case in the simulation in TRNSYS. During the simulation of the base case different parameters were varied and the results studied to find the most suitable storage design. The borehole configuration was simulated while holding the borehole storage constant. Number of boreholes and their spacing are important design parameters and were varied and their affect analyzed.

3.1.1. Mode 1: Solar ground thermal storage

The solar ground thermal storage mode is in operation during the storage period. Recharging the ground storage with heat is the purpose of this mode. Solar thermal energy from the solar collector is transferred to the water tank. The working fluid is water in both loops. The hot water from the solar collector then heat transfer with the cold flow from the ground storage

loop in the water tank. The fluid on the load side then circulated through the boreholes. While hot water circulated through the boreholes a thermal energy is injected into the ground. The ground temperature will hence increase and this increasing tendency also increases the storage temperature. The storage temperature will continue to increase during the storage period. An ON/OFF differential controller is used to control the solar collector. Two circulation pumps are used to circulate the water in the two loops.

3.1.2. Mode 2: Solar direct heating

The solar collector mode is the first mode in operation when the storage season is over and heat demand for the building is present. The solar collector produces heat during the heating season increasing the water temperature in the tank. When the tank water temperature reaches 30-35^{o}C the water is high enough to be use for space heating. The coil-heating terminal will then receive hot water directly from the hot water tank. The hot water from the tank will heat exchanges with the air stream passing through the fan coil unit before entering the house. Floor heating, modern radiators and fan coils are low temperature system that makes it possible to utilize larger parts of the solar thermal heat.

3.1.3. Mode 3: Direct heat exchange with boreholes

When the temperature of the solar collector becomes too low to be used for direct heating in the system mode 3 should be set in operation. The boreholes have a high temperature after being recharged during the storage season. The boreholes are then ready to be used for direct heat exchange. The heat stored in the boreholes is extracted from the ground by the ground heat exchangers. The space heating requirements are in this mode covered by the borehole thermal energy storage.

There are two separate loops in this mode, the hot source loop and the cold load side. The hot waters stream from the borehole storage should have a temperature higher than 30°C for this mode to be in operation. The hot stream from the ground storage is exchanging heat with the cold airflow on thought he fan coil. The ground temperature has a decreasing tendency and will reach a pint where the temperature is not sufficiently high enough to singly cover the heating load. When the ground temperature reaches this point the heat pump is set in operation. It is favorable to use heat from the ground storage directly before introducing the

heat pump. This is done to avoid too high inlet temperature at the evaporator side while the operation time of the heat pump is decreased

3.1.4. Geothermal heat pump

The geothermal heat pump mode is the last mode. This mode takes effect when the temperature of the ground storage is too low for direct heat exchange. The heat pump is then set in operation and will utilize the remaining heat of the ground storage. The heat that is left in the ground storage may not be high enough for direct use but can be used as a heat source for the heat pump. Because of this extra heat from the ground storage the COP of the geothermal heat pump will be higher than for a normal geothermal heat pump without the extra heat supply. The compressor will need less work input since the ground is not unheated. Because of the solar collector the source temperature can be around 20-30^{o}C. For a system without the solar collector the source temperature will be equal the undisturbed ground temperature at the given location.

3.2. Geothermal heat pump

Heat pumps that exchange heat with the ground are classified as geothermal heat pumps. A geothermal heat pump can use the whole range of temperature and are distinguished in three categories according to temperature. This is high temperature, medium temperature and low temperature heat source. High and medium temperature heat sources are often the product of the thermal flows provided by the molten core if the earth. The ambient temperature is the temperature near the low temperature heat source. For solar energy incident on the ground and ambient air the low temperature heat source is applicable. Heat pump extract heat from lower levels and increases the temperature until it is sufficiently high for practical use. In this thesis the heat pump increases the temperature of the solar collector and stored as thermal heat in the ground storage.

There are two ways for the heat to be extracted from the ground, this through either an open loop system or a closed loop system. Throughout this thesis an open loop is chosen. In a closed loop system the fluid will never be in any direct contact with the surrounding ground and the working fluid circulates in an enclosed loop. There are two different closed loop systems; these distinguished by the orientation of the heat exchange pipes. The two systems are vertical and horizontal closed loop systems.

3.2.1. Vertical closed loop system

As the name implies a vertical closed loop system has vertically oriented heat exchange pipes. Pairs of pipes are connected at the bottom by a U-shaped connector and are bored down in the ground. As the heat exchangers are placed vertically the installation area are reduced giving this system a huge advantage. Due to the small surface ground area required this system has more placing choices and can be used when the available surface area is limited. As discussed in section 6.4 the ground temperature remains stable when you reach a certain depth, the fact that the ground temperature is unaltered by seasonal variations is another advantage with a vertical design. This can reduce the length of the loop and the heat pump will have a more stable performance. Drilling is performed when installing the vertical loops. Compared to trenching, which are used for horizontal loops, drilling is space reducing but the costs of drilling is high.

3.2.2. Horizontal closed loop pump

With a horizontal design the ground loop is laid out horizontally not exceeding couple of meters below the ground surface. The loop is laid with backfilled trenches and is most commonly used where the available space is not limited. Since the ground loop is highly influence by yearly and daily weather variations the ground loop is laid below the frost line where frost is represented. The soil is varying with the ambient temperature and the heat transfer will be affected by these changes. Longer pipes are needed due to the influence from the thermal properties of the soil that fluctuates with rain, snow, vegetation and shades. The working medium in a horizontal closed loop consists of a mixture between water and antifreeze to avoid freezing during cold seasons. The pumping energy will be increased dude to the viscosity of the antifreeze; this will in turn decrease the overall heart transfer and thus the overall system efficiency.

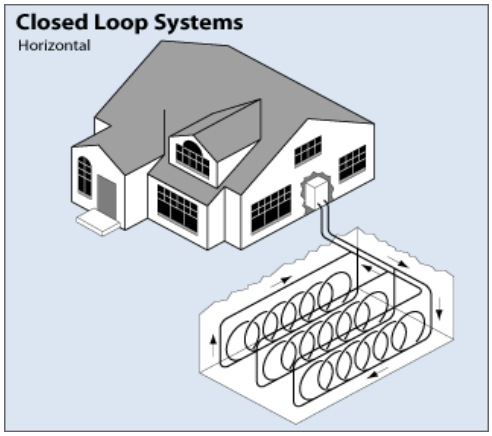

Figure 6: Horizontal closed loop system

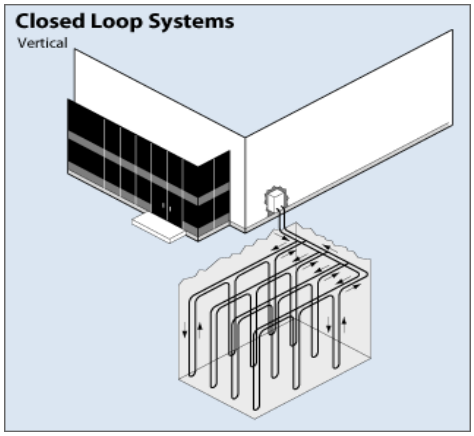

Figure 7: Vertical closed loop system

3.2.3. Working principles

In a closed heat pump the heat is transferred and transported by the refrigerant. Water is used as the refrigerant in this system. In short the heat pump compresses the refrigerant to make it hotter on the heat sink side while the pressure is released at the source side where the heat is absorbed. The main components in a heat pump are the compressor, expansion valve, condenser and evaporator.

The working fluid, in its gaseous state, is pressurized and is circulating through the system by a compressor. In the compressor the volume is increased and likewise the pressure and temperature are increased. The now highly pressurized vapor continues to the heat exchanger, condenser, where it is cooled down. In the heat exchanger the heat is exchanges with the heating system, and the working fluid is condensed into a high pressure, moderate temperature liquid. The refrigerant is at higher temperatures than the room temperature; this gives heat transfer from the refrigerant to the room.

After exchanging its heat the working fluid passes through a pressure-lowering device. This is often an expansion valve where the temperature and pressure is decreased. The real heat gain takes place in the evaporator where the working media is brought form a low temperature up to a high temperature, by absorption of heat until boiling. The heat from the ground loop is transferred to the evaporator. Now the working fluid takes up heat again from the environment, and the cycle begins over again.

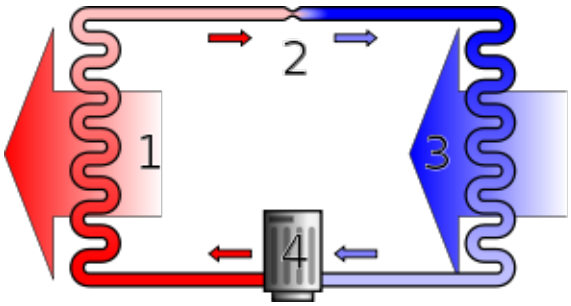

Figure 8: Water circulation through a heat pump, 1. Condenser, 2. Expansion valve, 3. Evaporator

3.2.4. COP – predicting the performance

The Coefficient of Performance (COP) is defines as the ratio of the heat output to the amount of energy input of a heat pump at given conditions. The COP of a heat pump is an important parameter and it is used to describe the performance of the heat pump. If the COP is greater than one it implies that the amount of useful energy delivered from the heat pump is greater that the amount of input net work.

$$COP = \frac{Q_{load}}{W_{cycle}} = \frac{Q_{load}}{Q_{load} - Q_{source}} = \frac{T_{load}}{T_{load} - T_{source}}$$

Equation 1: Coefficient of Performance (COP)

Q_{load} The amount of useful energy discharged from the heat pump system [kJ]

W_{cycle} The net work provided into the system [kJ]

Q_{source} The energy drawn from the surrounding atmosphere [kJ]

3.3. Solar collector

The solar collector is the key part in a solar thermal heating installation. When selecting the type if solar collector one should base it on the quantity and quality (temperature) of the demanded heat [10]. If you intend to use the solar collector for domestic hot water and space heating systems the glazed flat plate and evacuated tube collector are the most relevant options. The heat gain and loss mechanisms in different collector types are the same [19] .It is normal to differentiate between the optical losses and the thermal heat losses due to different transfer mechanisms for the different collector types. Absorber, cover and insulation are typically the three main parts of a solar collector.

3.3.1. General construction of a solar collector

The absorber collects the radiation from the sun before it is carries away by the fluid flowing through the tubes. The tubes are attached to the absorber. Solar collectors are located outside to absorb the heat from the sun. When located outside, the solar collector is affected by the metrological conditions at its given site. The surrounding environment will create heat losses due temperature differences. The ambient air will in most cases be lower than the collector temperature. Insulation is placed on the side and back of the absorber while a cover is placed on the front, this to minimize the heat losses to the surroundings. The cover placed on the front of the absorber must allow the solar radiation to come through. Short wave radiation passes through the cover while long waved radiation is trapped inside, increasing the efficiency. The cover is usually made of glass or plastic consequently reflecting parts of the incoming solar radiation back to the atmosphere. Finding an optimal solution between reducing the heat losses and reducing the transmission capability will always be a challenge.

Solar radiation is converted into heat by the absorber and thus the absorber is the most important part of a solar collector. The absorber if often coated by coating with a high absorption coefficient, a, too maximize the amount of energy collected. Absorptivity is the fraction of incident sunlight captured by the collector [19]. The absorbed radiation sets the molecules on the surface in motion, and radiation energy is converted into thermal radiation.

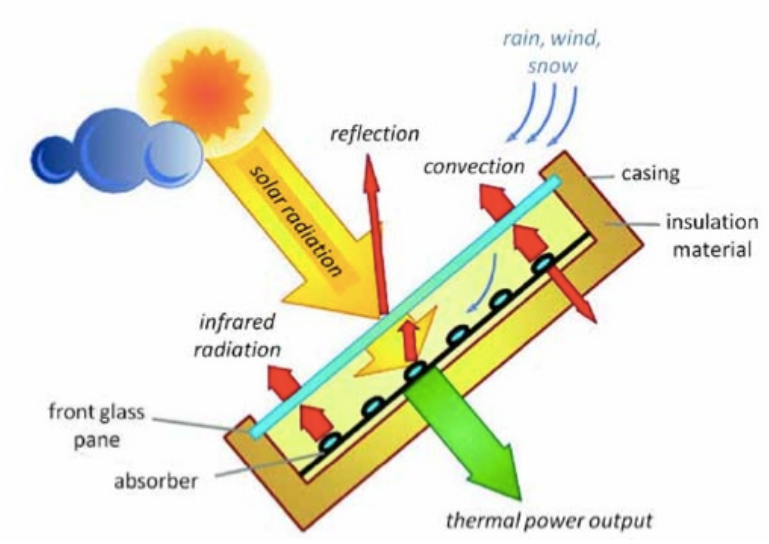

Figure 9:Principal sketch of a solar collector

3.3.2. Evacuated tube solar collector

In the system used in this thesis an evacuated tube solar collector is chosen. Evacuated tube collectors can raise the temperature to as high as 177 ˚C [19]. They encase the absorber surface and the tubes of the heat transfer fluid in a vacuum-sealed tubular glass for highly efficient insulation. When the climate is cold and there are low levels of diffuse sunlight an evacuated tube solar collector is the most efficient type. Among the evacuated tube collectors we find three types: Direct flow evacuated tube solar collector, heat pipe solar collector sydney tube type evacuated tube solar collector

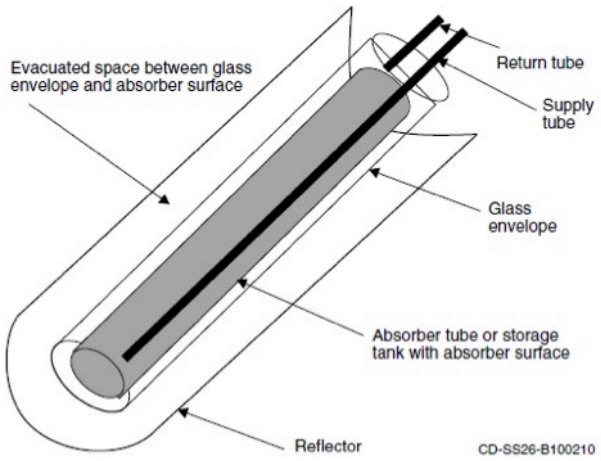

Figure 10: Sketch of an evacuated tube solar collector

The different evacuated tube collectors are described above, but they all have certain qualities in common.

- All evacuated tube collectors consist of several evacuated glass tubes placed in parallel. They are all attached by an insulated diversity at one end for supply and heat removal transfer fluid.
- Heat losses caused by conduction and convection are small due to the vacuum insulation.
- The “header” is connected to the upper end of the tube.
- To endure the outside pressure the tubes have a circular shape.

An evacuated tube solar collector is most commonly used when there is use for hot water to cover domestic hot water heating. For applications that have cooling in the summer and where buildings have heating need hotter water is required.

3.3.3. Collector efficiency and solar fraction

The solar collector efficiency is directly related to the heat losses from the surface of the collector. The thermal gradient between the temperature of the collector surface and the ambient temperature govern the heat losses and thus the efficiency itself. When the collector surface temperature increases or the ambient temperature gets too low the temperature difference will increase resulting in higher losses and lower efficiency. By increasing the insulation of the collector the decrease in efficiency can be diminished. For an evacuated tube collector a vacuum seal would be used as insulation.

The solar fraction is used to analyze how the solar system performed technically. As seen from *Equation* 2, the solar fraction is defined as the amount of energy provided by the solar system divided by the total thermal load of the building.

$$SF = \frac{E_s}{E_{building}}$$

Equation 2: Solar Fraction (SF)

E_s Total amount of solar energy provided by the heating [kJ]

$E_{building}$ Total heating demand of the building [kJ]

3.4. Stratified water tank

A stratified water tank is used as a buffer tank in systems where the energy source is somehow unstable. This is usually when there is a mismatch of supply and demand, like in a solar system. To gain stability in the system energy storage units are of great importance. The stratified water tank will be used to handle the peaks in delivery from the solar collector when the heating demand possibly will not be as high. The water tank is directly connected to the solar collector. The BTES or the buffer tank supplies the heat distribution; because of limited charging and discharging powers of the BTES a buffer tank is essential. In times when the tank temperature is high enough it will be used for supplying heat to the heat distribution system. In times when the temperature is not adequately high enough solar heat will be uses for the water to reach the necessary temperature.

A stratified water tank has cold water at the bottom while the hot water is placed at the top of the tank. Another water tank type is a fully mixed tank. In a fully mixed tank the hot water from the solar collector and the cold water in the tank is mixed.

Stratification is made possible by the gravity and buoyant effect created by the temperature and density. Hot water and cold water will have different density. The hot water will float to the top off the storage due to its lighter density; the cold water with higher density will sink to the bottom. This creates a storage containing different thermal zones. The temperature gradient in the tank or thermo-cline is formed between the hot and cold water within the tank.

In the proposed heating system the cold water from the tank is extracted at the bottom and fed directly to the solar collector. The water then circulated through the solar collector where it is heated before returning to the water tank. The load is supplied by hot water from the top of the tank in the second circuit. After supplying the load the water in the second circuit returns as cold water to the bottom of the tank. When the cold water flows downward in the tank it can cause mixing and destruction of the thermal stratification, this due to turbulence that may occur.

4. Description of the TRNSYS Software

This section introduces the simulation software TRNSYS and its connected building creator program TRNBuild. Further the concept house and its parameters and characteristics are presented. The buildings properties and creation is described. Two locations are used for this heating system in order to compare different aspects and moreover the weather conditions for the two areas are described below.

4.1. TRNSYS

Simulation has become an influential tool since it gives the opportunity to estimate and calculate important values. By estimation real life conditions it is a great help when planning energy systems for a building. The University of Wisconsin at Madison developed the simulations software TRNSYS [20]. TRNSYS is a tool used for building energy analysis and is used in this thesis.

TRNSYS [20] is used to simulate the different modes in the energy system. TRNSYS is a modular system simulation package in which the user describes the components that comprise the system and the manner in which these components are interconnected. The user can change different parameters and variables of the components. This flexibility allows the user to explore new systems in an easy way. The effect of the different components behavior within the system can then be analyzed. Type 56 describes a building with multiple thermal zones and walls with different thermal properties, and is used to represent the concept-house in TRNSYS. This building file is created within the sister program to TRNSYS, TRNBuild.

A vertical U-tube ground heat exchanger is used to simulate the BTES. The GHP was modeled using a water-to-water heat pump. In Appendix B. the different TRNSYS components used in the models are listed.

4.2. Introduction to the concept house and location

4.2.1. TRNBuild

TRNBuild is the part of TRNSYS used to create the building file used as a load in the simulation. Different thermal zones, representing different rooms or floors, are construct in the TRNBuild file. There are four different kinds of construction elements in the building file: external walls, floor, windows and roof [20]. The concept-house is treated as one simple zone

with a single inside air temperature [20]. The thermal properties for the building shell and frame were chosen to equal a typical single-family house [21]. The thermal properties as well as the heat gains from the occupants and lightning in the building were implemented in the file.

4.2.2. Heat flows

The heat flow within the building is calculated from Equation 3. This calculation is performed for each time step.

$$Q_{internal} = Q_{conv,surf} + Q_{conc,infil} + Q_{conv,vent} + Q_{conv,adj.space} + Q_{conc,int} + Q_{rad,solar}$$

Equation 3: Heat flows within the building zone

$Q_{internal}$ total heat flux into the thermal zone [kJ/hr]

$Q_{conv,surf}$ surface convection from walls[kJ/hr]

$Q_{onv,infil}$ convective heat gains from infiltration[kJ/hr]

$Q_{conv,vent}$ convective heat gains from ventilation[kJ/hr]

$Q_{conv,adj\ space}$ convective gains form adjacent zones[kJ/hr]

$Q_{conv,\ int}$ heat gains created within the zones [kJ/hr]

$Q_{rad,solar}$ radiative heat gains[kJ/hr]

4.3. Building layout and properties

The Concept-house is not yet occupied and no experimental data have been recorded yet. For this study the Concept-house is considered as a normal residential building where people will be working and living in on a daily basis.

Initially occupant schedules and the internal gains are setup for a normal residential dwelling. The house consists of two floors, where the first floor is located at the ground and the house has a colt attic. The concept-house is a standard single family home with a typical town house design. The measurements of the concept-house are listed in the table below; the parameters are given for one floor. The concept house consists of two equally designed floors and a cold attic. The attic will have no heating and works as an adjacent layer for the roof of the house.
To receive the right data from the concept-house the different material used in the building must be added to the building file in TRNBuild. The building materials used in TRNBuild for the concept house are listed in Table 1.

Table 1:Building Parameters

Buildings shell component	Total thickness [m]	U-value [W/(m2K)]	TEK07 (Norwegian regulations) [21]
External walls	0.256	0.202	0.18 (0.22)
Floor	0.27	0.174	0.15 (0.18)
Roof	0.240	0.16	0.13 (0.18)
Window		1.24	1.2 (1.6)

The layout of the concept house is somewhat simplified. The total volume of the house is 640 m^3. Table 2 provides an overview of the building major characteristics.

Table 2: The buildings major characteristics

Floor area	128m^2
Height	2,5m
Length	16m
Width	8m

The building shell and illustration are given in Appendix A. and are used as input parameters in the building file. The concept house is broken down to individual walls/plates with different structure.

4.4. Weather Conditions

The weather model in TRNSYS is used to obtain the solar radiation and metrological data for different locations. Meteonorm provides the metrological data used in the weather component in TRNSYS. They have stations worldwide providing metrological data for more than 150 countries [22]. Norway is also represented, where a station located at Trondheim provides the metrological data.

In this paper two cities will be evaluated, on located in the northeast if China and one city located in Norway. The city located in China is Changchun represented by a weather station located in Siping.

4.4.1. Weather conditions and demography for Norway

Norway or the Kingdom of Norway is located on Scandinavia north in Europe. It is located at 59°56′N 10°41′E. Norway has a total area of 385 178 km^2 and in 2013 the country had a population of 5 136 million people. Norway is located in the cold climate region, but with the warm Gulf Stream in the Atlantic the temperature and climate is milder than in countries placed equally far north. Norway is known for its long coastline and high mountains. This results in a varying climate throughout the country. In the northern part the climate is more arctic, continental in the east and typically maritime in the west. In the northern part the days are short in the winter due to the Arctic Circle. This results in a larger heating demand during the winter months. Due to global warming the temperature has increased in Norway resulting in an increasing cooling demand in the summer months.

Meteonorm provides weather data from a weather station located in Trondheim. Trondheim is a city county located in South Trøndelag municipality. It is the third largest municipality in population with 182 513 inhabitants. It has a total area of 342 30 km^2 and is located at 63°25′47″N 10°23′36″E.Trondheim has a mild and humid climate that is due to the cities location at the edge of eastern seaboard. The location between the warm air in the south and the cold in the north provides a rapidly changing and unstable climate. The city is in the temperate climate zone, the part located by the fjords experience a milder climate while the part further north experience a colder climate.

4.4.2. Weather conditions and demography for China

China can be divided into five climate zones. These zones are used in China's building energy standard. The different zones are (1) severe cold, (2) cold, (3) hot summer and cold winter (4), and (5) hot summer and warm winters.

The heating and cooling trends can be seen from the zones. In the northern part of Chine where we find the severe cold and cold zones have a large heating demand due to the cold climate. The central part of China is located in the hot summer and cold winter zone. This

results in both a demand for heating and cooling in residential buildings. In the south part of China we find the hot summer and warm winter zone. Building located in this area will have a high cooling demand during the hot summers.

Changchun is the capital of the Jilin province (climate data of Siping), located in the northeast of China. It is located at 43°54′N 125°12′E. It has an area of 20 532km^2 and a population of 7 459 million people in 2010. The city is situated in the eastern part where there are small areas of low mountains. The climate is humid, they experiences four-seasons and monsoons. The winters are long, cold, windy and dry while spring and fall are dry and windy. The summers are hot and humid.

5. Base Case Parameter

In this thesis a base case is used as a stepping-stone for the system optimization. In this section the parameters used as the base case are presented.

Table 3:Parameters base case

Characteristics	Value	Comments
Solar Collector		
Number in series [-]	1	
Collector area [m^2]	200	Based on simulations, high enough storage end temp.
Fluid specific heat [kJ/kgK]	4.19	Specific heat for water
a_0[-]	0.839	Given by the producer
a_1[kJ/hrm^{2}K]	3.200	Given by the producer
a_2 [kJ/hrm^{2}K^2]	0.0137	Given by the producer
Mass flow [kg/hr]	330	
Water Tank		
Source (solar collector flow) specific heat [kJ/kgK]	4.190	cp for water
Load (storage loop flow) specific heat [kJ/kgK]	4.190	cp for water
Tank volume [m^3]	20	
Tank loss coefficient [kJ/hrm^{2}K]	2.5	
Ground Storage		
Ground		
Initial temperature [°C]	5.1	Annual average air temperature in Trondheim, Norway
	7.1	Annual average air temperature in Siping, China
Thermal conductivity [kJ/hrmK]	5.22	

Heat capacity [kJ/m^3/K]	2016	
Boreholes		
Borehole radius [m]	0.15	
Number [-]	6	
Number of boreholes in series [-]	2	
Borehole depth [m]	30	
Borehole flow rate [kg/hr]	1059.75	Measured in earlier experiments
Borehole spacing [m]	2	
Storage volume [m3]	623.45	V = π*number*depth*(0.525*spacing)^2
Soil temperature [°C]	7.1	Trondheim
(souce)	9.1	Siping
Insulation thickness [m]	1	Simulated, reduce storage losses (side)
Ground Heat Exchangers		
Inner radius of U-tube pipes [m]	0.013	
Outer radius of U-tube pipes [m]	0.016	
Number of U-tubes per borehole [-]	1	
Pipe thermal conductivity [kJ/kgK]	1.656	Pipe material is polyethylene
Fluid specific heat [kJ/kg]	4.19	cp for water
Fluid density [kj/m^3]	1000	Density of water
Pumps		
Rated power [kJ/hr]	2684	
Total pump efficiency [-]	0.6	

6. Simulation and results

In the subsequent section results obtained during TRNSYS simulation are presented and discussed. Operation mode 1, the storage mode, are simulated and presented first. Results and the optimized operation parameters for Trondheim and Siping are provided. Afterward the three different heating modes are simulated and results obtained. Following the simulation results from the heating modes are discussed and the entire system, including the storage mode, are analyzed. The electricity use and the COP are presented.

6.1. Temperature and radiation

The temperature over the duration of a year can be seen in Figure 11 and Figure 12, the temperature is low in the winter and high in the summer. This means that the energy demand will be high in the winter and low in the summer. The solar radiation has the opposite tendency, with high solar radiation in the summer and low in the winter. This mismatch in supply and demands makes a seasonal storage suitable

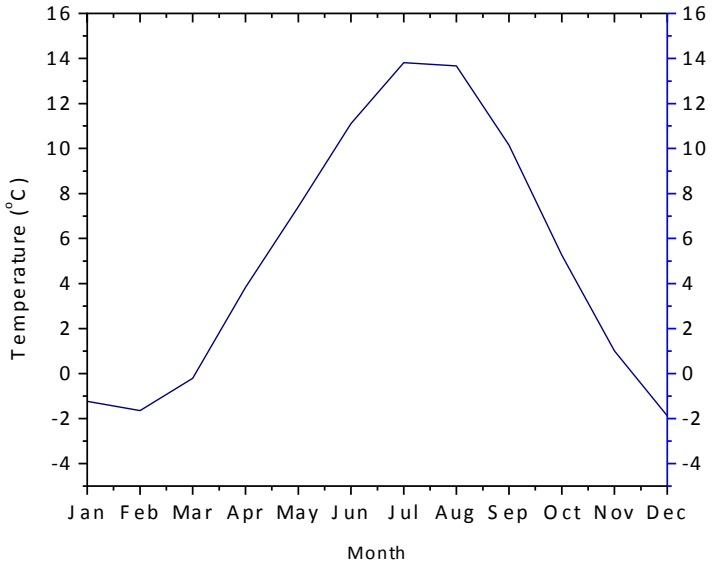

Figure 11: Monthly average temperature Trondheim, Norway

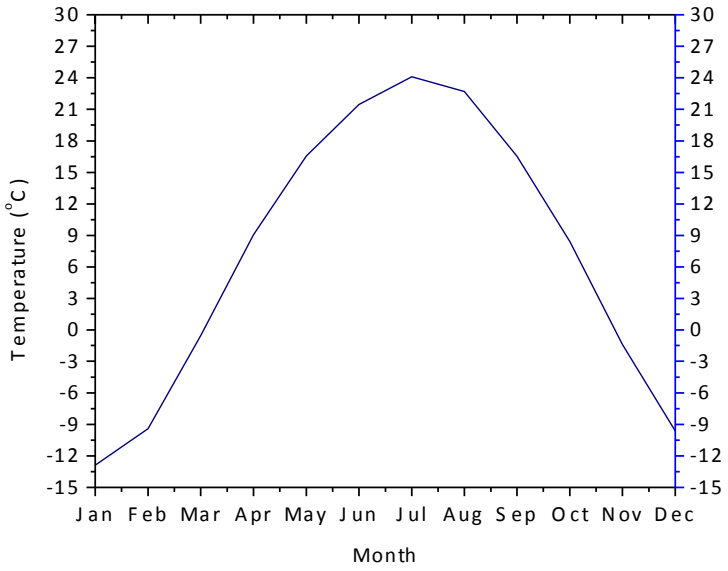

Figure 12:Monthly average temperature Siping, China

The temperature profiles of the two different locations show that they both experience cold temperatures in the winter and increasing temperature during the summer. Their profiles differ from each other and it can be seen from Figure 11 and Figure 12 that Norway has a lower average temperature compared to Siping. Norway has a low average temperature of 5.1^{o}C while Siping experiences an average temperature of 7.19 ^{o}C [23]. Siping has a higher variation between the high and low temperature months. Even though Siping has a higher average ambient temperature the winters are colder and summer wormer than for Trondheim.

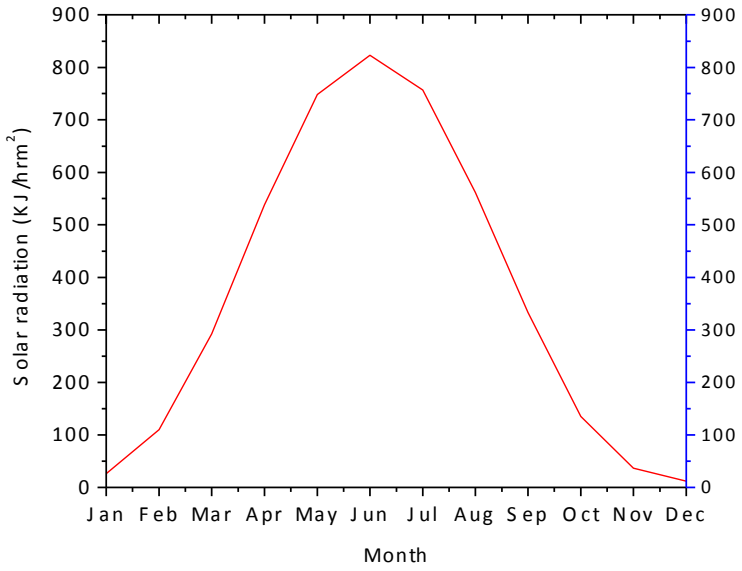

Figure 13: Monthly average solar radiation on horizontal plate Trondheim, Norway

Figure 13 show how the monthly average solar radiation for Trondheim vary over a year. It can be easily seen that the solar radiation is highest in the summer months and decreases towards the winter. The radiation in Trondheim is high at its peak in June but decrease significantly and becomes low over a long period. Norway experiences almost zero radiation in the winter months December and January.

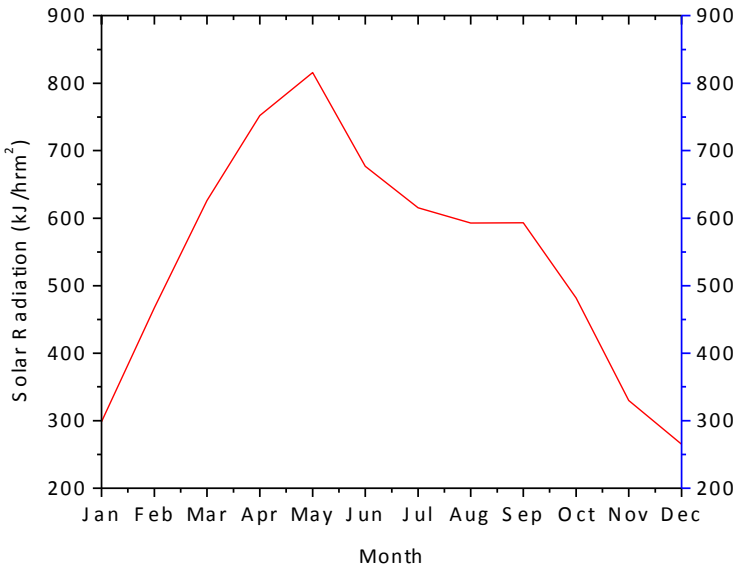

Figure 14: Monthly average solar radiation on horizontal plate Siping, China

From Figure 13 and Figure 14 it can be seen that the solar radiation in Norway differs in many ways from the solar radiation in Siping. Norway has an overall lower solar radiation throughout the year. The solar radiation curve has higher increase towards the summer months and a longer period of low radiation. The two cities located in China have both an overall higher radiation in the winter months. Norway experiences almost zero radiation in the winter months December and January, while the solar radiation in China is still well represented.

6.2. Simulation of the concept house

The heat demand of the concept house was simulated in TRNSYS. The heating demand of the concept house is used as the heating load during the heating modes. The concept house is a small town house, described in Section 4.2. The simulated living area comprises an area of 128m^2, representing a fairly small single residential building. The simulated living area comprises s 128m^2 representing a fairly small single residential building. The volume is 640m^2 and the house as mentioned previously is considered as one single thermal zone. To perform the simulation of the house its building material, internal gains, dimensions, distribution and orientation need to be used in TRNBuild.

Figure 15 and Figure 16 show the heat power demand for each moth over one year for Trondheim and Siping respectfully. The figure show that the heating demand varies with the ambient temperature and the prevalent heating demand is found in the cold winter months. The heating season is found to be from June to August for Trondheim and from May to September for Siping. The heating and storage months are presented in Table 5.

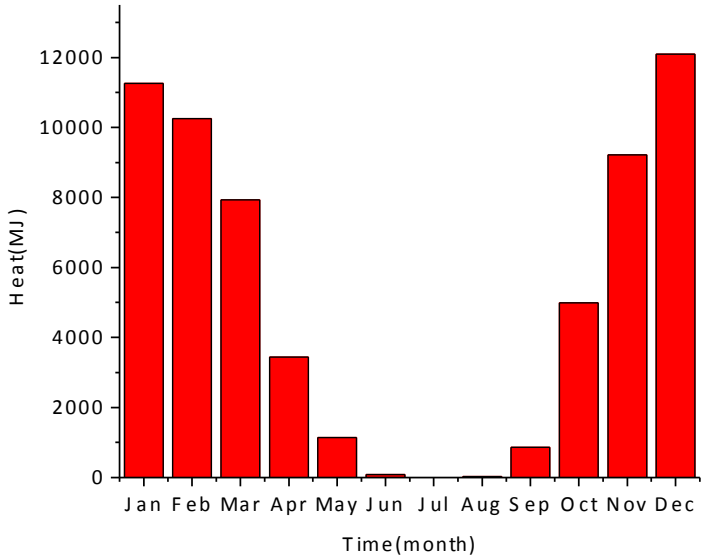

Figure 15: Heat load characteristics for the concept house located in Trondheim, Norway over a year

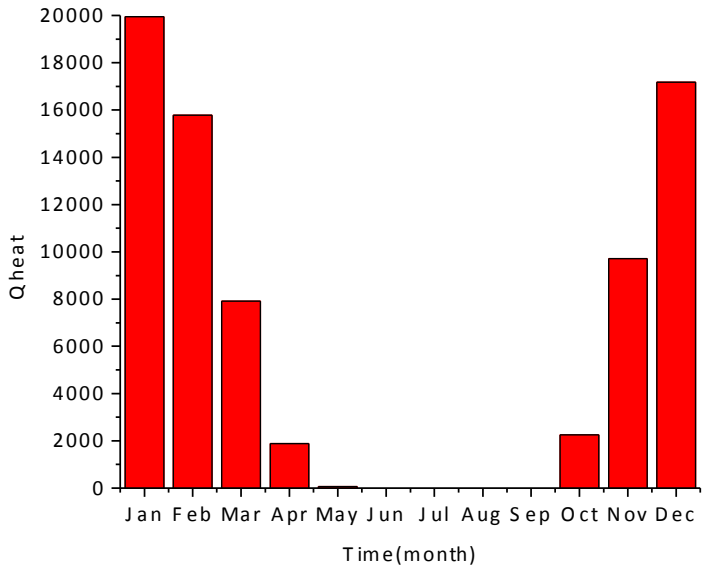

Figure 16: Heat load characteristics for the concept house located in Siping, China, over a year

Table 4: Overview of the power demand for the space heating of the concept house for Trondheim and Siping

	Yearly heat demand (kJ)	Average heat demand (kJ/hr)	Peak power demand (kJ/hr)
Trondheim	44553968.23	5085.49	24625.46
Siping	54222310.15	6189.05	33085.13

	Yearly heat demand (W/m^2)	Average heat demand (kJ/hr m^2)	Peak power demand (kJ/hr m^2)
Trondheim	98.69	39.73	192.39
Siping	117.67	48.35	258.48

In the previous section, 6.1, the ambient temperature and solar radiation over a year was simulated for the two locations. The behavior of the ambient temperature and the solar radiation at the given location has a large effect on the heating demand. Seen from Table 4 the yearly heating demand for Siping is higher than for Trondheim. Norway has a heating demand that is present almost every month throughout the year due to low yearly radiation and a low average ambient temperature. Siping experiences very low temperatures in the winter months giving a high heating demand. In January the heating demand in Siping is almost the double of what it's found to be in Trondheim. However, from May to Sept the house has no heating demand due to a high ambient temperature and radiation. Even so the yearly heating demand is higher for Siping than for Trondheim due to the high demands in the winter months.

Table 5: Heating and cooling seasons

	Heating period [Month]	Storage period [Month]
Trondheim	Sep-May	Jun-Aug
Siping	Oct - Apr	May - Sept

6.3. Simulation of Operation mode 1: The solar thermal ground storage mode

The first operation mode is as previously explained the only storage mode, the solar thermal ground storage mode. Table 3 presents the different parameters used as a base case for this simulation. The aim is to design a solar thermal ground storage that is able to store a large amount of heat and achieve a sufficiently high storage temperature in the end of the storage season. This so the ground storage fulfills the requirements for further operation of the heating modes and building demand.

There are two closed loops in this storage mode where the working fluid circulates. The blue is the solar collector loop, and the green represents the ground storage loop. As seen from Figure 17 there are two pumps in the system each used to circulate the working fluid in each loop. The controller is used to control the operation time of the solar collector.

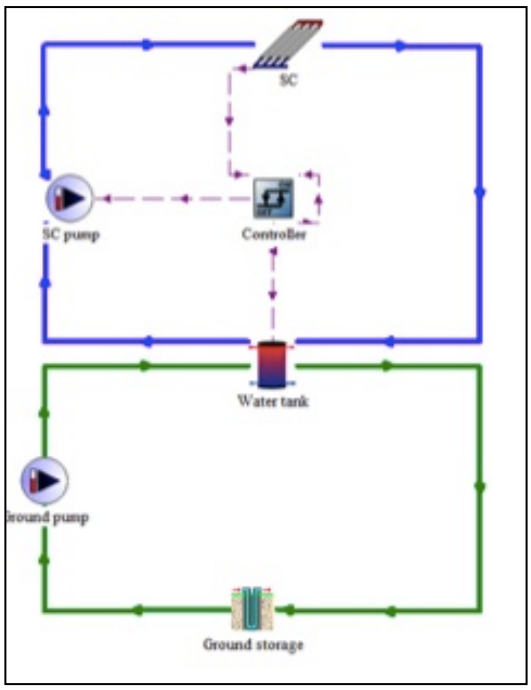

Figure 17: Simplified TRNSYS screenshot of operation mode 1, Solar thermal ground storage

Table 6: Operation scheme for heating mode 2

Operation mode	Solar collector	Borehole
1.Solar underground thermal storage: In operation during the storage season. Heat is absorbed by the solar collector is transferred to the water tank before injected into the ground storage.	Solar collector used to recharge the boreholes.	Heat is injected and stored in the boreholes. Increasing temperature gradient within the storage.

6.3.1. Investigating the behavior of the Solar Collector and efficiencies

The solar collector area is an important parameter in a sola collector system. The collector area determines the amount of received solar radiation, which in turn gives the amount of useful energy that can be utilized by the system for heating. The thermal efficiency of the solar collector is a parameter of great importance. To estimate the thermal efficiency the different energy flows within the solar collector has to be considered.

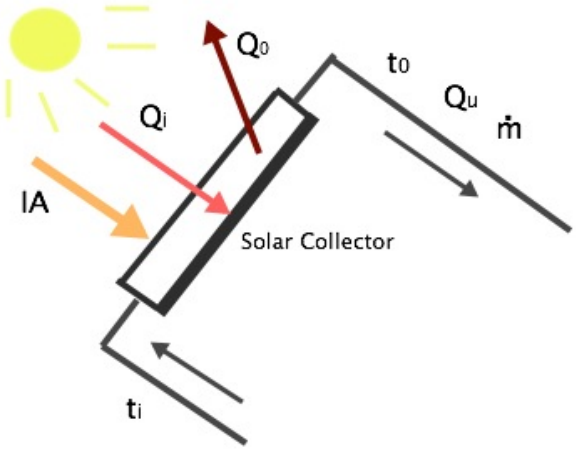

Figure 18: Illustration of the solar collector gain and losses

The amount of solar radiation received by the collector is represented by Q_i[kW] and given by Equation 4:

$$Q_i = I(\tau a)A$$

Equation 4: The amount of solar radiation received by the collector

Q_i Collector heat input [kJ]

I Solar radiation per square meter solar collector [kJ/hrm^2]

A Surface area of the solar collector [m^2]

τ Transmission coefficient of glazing [-]

α Absorption coefficient of plate [-]

The solar radiation that reaches the solar collector area is with an energy amount of IA. The collector absorbs not the entire amount of solar radiation that strike the collection area. Some of the solar radiation is reflected back to the sky while the cover absorbs an additional part. The amount left is transmitted through the cover and reaches the absorber. This amount will be the amount of useful solar energy, the energy that can be consumed by the system. The parameters $\tau\alpha$ represent the transmission rate of the cover, and the absorption rate of the absorber. This factor indicated the percentage of the solar rays that are penetrating the cover and the percentage being absorbed.

When the solar collector absorbs heat the collector temperature rises consequently. This leads to a temperature difference between the collector and the ambient temperature. Heat is then lost to the surroundings through convection and radiation. In addition to the temperature difference the heat loss coefficient also influences the heat loss. The heat loss Q_o is the amount that is lost in the solar collector and is given by Equation 5.

$$Q_u = UA(T_c - T_{amb})$$

Equation 5: Amount of heat loss in the collector

Q_o Heat loss [kJ]

U Collector overall heat loss coefficient [kJ/hrm^2]

T_c Collector average temperature [C]

T_{amb} Ambient temperature [C]

The useful energy gain, Q_u, is estimated from steady state conditions. The useful energy gain is the amount of heat-absorbed bye the solar collector minus the heat loss to the environment. The useful energy gain then becomes Equation 6

$$Q_u = Q_i - Q_o = I(\tau a)A = UA(T_c - T_{amb})$$

Equation 6:Useful energy gains

The fluid that circulates in the solar collector loop is carrying the useful energy gain. Equation 7 can measure the useful energy gain by the mass flow:

$$Q_u = mc_f(T_o - T_i)$$

Equation 7**:** Useful energy gains by mass flow

m Mass flow rate of the fluid flowing through the collector [kg/hr]

c_f Specific heat of the fluid following through the collector [kg/kgK]

T_0 The outlet temperature of the solar collector [C]

T_i The inlet temperature of the solar collector [C]

The collector efficiency is the ratio of the useful energy gain to the incident radiation over a given time period expressed by Equation 8:

$$\eta = \frac{\int Q\, dt}{A \int I dt}$$

Equation 8: Collector efficiency

$$\eta = \frac{Q_u}{AI}$$

Equation: 9: Instantaneous thermal efficiency

$$\eta_{s\_sys} = \frac{E_u}{AG}$$

Equation 10:Thermal efficiency

G Total solar radiation on the solar collector [kJ]

Equation 10 shows the system efficiency. The system efficiency is the ratio of the total amount of useful solar energy gain ant the total amount of solar radiation on the solar

collector over a period of time, calculated here over a period of 24 hours (one day in of operation) in Appendix G.

In TRNSYS and other simulation programs Equation 11 calculates the thermal efficiency

$$\eta = a_o - a_1 \frac{\Delta T}{I} - a_2 \frac{\Delta T^2}{I}$$

Equation 11:Thermal efficiency from TRNSYS

ΔT	$T_i - T_s$
a_o	The efficiency without the heat losses
a_1	The first order of heat loss coefficient
a_2	Second order of heat loss coefficient

The parameters a_0, a_1 and a_2 define the thermal efficiency and are provided by the solar collector producer. The working fluid in the solar collector loop is water and Equation 12; calculates the mass flow of the working fluid:

$$\dot{m} = \rho A v = \rho_{water} \times \pi \times r^2 \times \mathrm{v}$$

Equation 12: Mass flow of the working fluid

P	Density of the working fluid [kg/m^3]
A	Flow area [m^2]
v	Flow velocity of the fluid [m/s]

The following equations describe the connection between the different energy flows present in the storage model:

$$Q_u = Q_{load} - Q_{tl}$$

$$Q_{load} = Q_{inj}$$

$$Q_{inj} = Q_{store} + Q_{sl}$$

Q_u Useful solar energy gain [kJ/hr]

Q_{load} Rate at which sensible energy is removed from the tank to supply the load [kJ/hr]

Q_{tl} Rate of energy loss from the tank to the surroundings [kJ/hr]

Q_{inj} The rate at which heat is added to the ground storage volume from the fluid [k/hr]

Q_{stor} The actual rate at which heat is stored in the ground storage volume [kJ/hr]

$Q_{s;}$ The rate at which heat is lost to the ambient through the ground storage volume [kJ/hr]

Table 7: Efficiencies and rates with varied collector area

Results	Solar collector area [m2]					
	100	150	200	250	300	350
F_{StU}	52.88	53.27	53.43	53.50	53.40	53.04
F_{StL}	66.19	65.98	65.80	65.64	65.43	65.09
F_F	7.09	7.60	7.86	8.017	8.51	9.58
F_{LU}	33.68	33.80	33.94	34.07	34.17	34.27
24hr						
Tank efficiency	15.018	26.50	32.34	35.91	38.42	40.26
Thermal efficiency	19.07	27.43	35.03	41.98	48.24	54.03
Efficiency	16.52	14.55	12.36	10.97	9.69	8.43

The collector efficiency is decreasing with an increasing solar collector area, seen from Table 7. This is due to the increasing operation temperature. When the collector area increases more energy from the sun is absorbed due to a larger absorption area. This increases the temperature that the solar collector operates under. The tank efficiency will increase since the tank losses increase with a higher tank temperature.

$$\eta_{tank} = \frac{E_{tl}}{E_{inj}}$$

Equation 13: Tank Efficiency

Since the tank efficiency increases with an increasing solar collector area it can be concluded fro Equation 13 that the temperature losses in the tank increases more than the amount of energy injected to the tank.

Equation 14 represents the storage efficiency. It can bee seen from Table 7 that the storage efficiency decreases with an increasing collector area. This is because the storage losses will increase more than the injected energy when the solar collector increases.

$$\eta_{storage} = \frac{E_{sl}}{E_{inj}}$$

Equation 14: Storage Efficiency

6.3.2. Sizing the Solar Collector area

The system was simulated with different solar collector sizes to determine what size to use for this system. The size of the solar collector area was varied from 100m^2 to 350m^2.

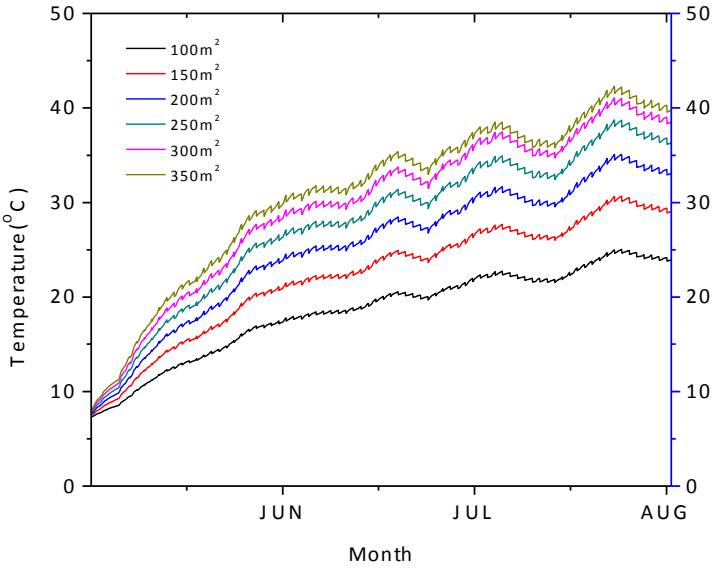

Figure 19: Storage temperature over the entire storage season with varying solar collector area in Trondheim, Norway

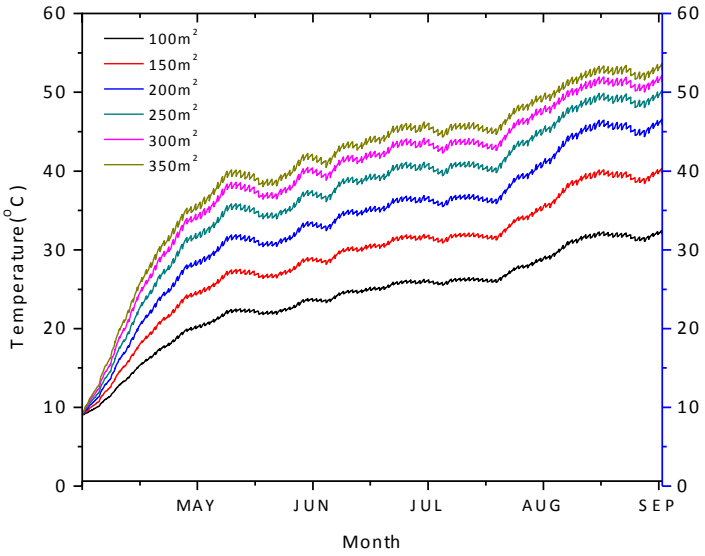

Figure 20: Storage temperature over the entire storage season with varying solar collector area in Siping, China

When the collector area is increase the storage temperature increases accordingly, this will result in higher temperature losses to the surrounding ground. In Figure 19 and Figure 20 this trend can be seen. The amount of stored energy increases with the collector area but the increase in stored energy decreases when the collector area gets larger. The increase in the

amount of stored energy from an area of 100m^2 to 150m^2 is much greater than the increase from 300m^2 to 350m^2, seen from Figure 21 and Figure 22. This is due to the increase in storage losses.

The amount of energy stored in the storage increases with an increasing collector area giving a larger collector area for solar energy. It can also be seen that the increase in the amount of stored energy reduces when the collector area get too high. When deciding the solar collector size one can argue that the amount of stored energy will increase with an increasing collector area and therefore a large collector area is beneficial. Space requirements and the economical aspect are not evacuated.

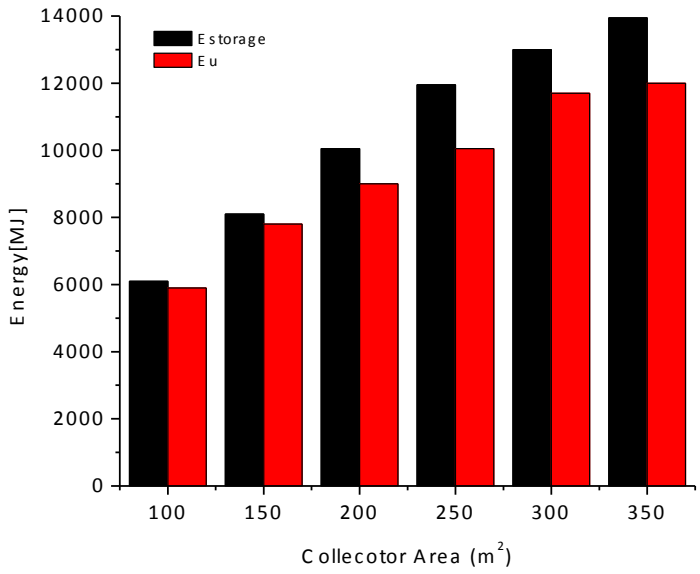

Figure 21: Stored Energy and useful energy with varying solar collector area, Trondheim

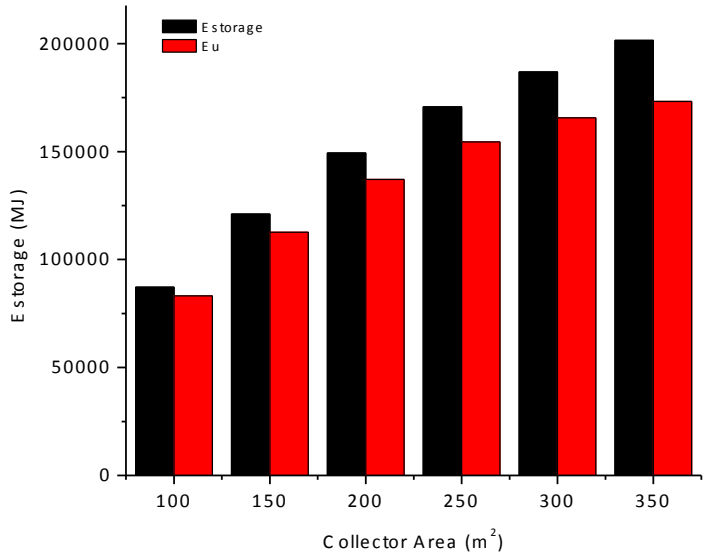

Figure 22: Stored Energy and useful energy with varying solar collector area, Siping

When the area of the solar collector is increased the total amount of useful solar energy gain and the total energy stored in the ground also increases, seen in Figure 21 and Figure 22. The rate of the energy injected into the storage volume is named Q_{inj}. Equation 12 gives Q_{inj}.

$$Q_{inj} = c_f Q_f (T_{fin} - T_{fout})$$

Equation 12: Rate of energy injected to the storage volume

Q_{inj} Rate of injected energy to the storage volume [kJ/hr]

m_f Mass flow of the fluid [kg/hr]

T_{fin} Inlet temperature of the fluid [^oC]

T_{fout} Outlet temperature of the fluid[^oC]

To evaluate the maximum amount of thermal energy that can be stored in the ground storage one has to look at the storage capacity.

$$C = \rho c_f V (T_{max} - T_{min})$$

Equation 13: Storage capacity

As seen from Equation 13, the capacity is dependent on the minimum and maximum average storage temperature. Then storage volume and heat capacity is also parameters of importance when calculating the capacity.

C	Storage capacity [kJ]
P_c	Storage heating capacity if the soil [kJ/m3K]
V	Ground storage volume [m3]
T_{max}	Maximum average storage temperature during one season [C]
T_{min}	Minimum average storage temperature during one season [C]

The difference between the stored heat and the useful energy gain increases with an increasing collector area seen in Figure 21 and Figure 22.

As discusses the storage losses increases when the storage temperature increases with the increasing collector area. The amount of heat stored is the amount of heat injected minus the storage losses.

$$E_{loss} = UA(T_{soil} - T_{amb})t_{year}$$

Equation 14: Storage heat loss

E_{loss}	Annual storage heat loss [kJ]
U	Equivalent mean storage heat loss factor [kJ/hrm^{2}K]
T_{soil}	Mean annual storage temperature [C]
T_{amb}	Mean annual ambient temperature [C]
t_{year}	Duration of one year [s]

Equation 14 expresses the storage heat losses. From the equation it can be seen that the storage losses are dependent on the mean annual storage temperature and the ambient temperature. The mean annual temperature is decided by the weather conditions at the location chosen for the system and is not affected by the system design. The mean annual storage temperature is highly dependent on the system design and an important value.

6.3.3. Designing the ground storage

The storage volume used in this system has a cylindrical chap where the depth, number of boreholes and spacing between the boreholes are parameter determine the size of the storage. Equation 15 expresses how the borehole volume is calculated.

$$V = \pi \times Number of Boreholes \times Depth \times (0.525 \times Spacing)^2$$

Equation 15: Borehole volume

It is important to size the system correct. The size of the system depends on the energy demand, the heat pumps operation time during a year and the desired temperature of the storage. The storage size has also a great influence on the drilling cost and the total cost of the system. In this case the storage size is based on the systems performance and not on the cost. To find the best ground storage design the depth, number of boreholes and spacing are varied and simulated.

Table 8: Initially properties for the BTES

Properties	Base Case
Number of boreholes [-]	6
Depth [m]	30
Pipe material [-]	Polyethylene
Volume [m^3]	623.45

Table 8 show the initially properties of the storage under investigation, however the entire base case is presented in Table 3.

The BTES should be designed with small spacing and shallow depth if the purpose is seasonal storage. There are not used any insulation in the BTES design or any special filling in the storage. The header depth is set to 1.5 meter since a depth less than 2 meter makes the ground highly influenced by the seasonal variations.

The borehole depth was varied between 20 - 100 meters. For small-scale use 10-50 meters are commonly uses. The storage depth was also set to 100m since the location is set to Norway where the ground temperature is low, and deeper boreholes may result in better operation.

Table 9: Borehole depth and storage volume, number of boreholes and spacing kept constant.

Borehole Depth [m]	Resulting Storage Volume [m^3]
20	415.63
30	623.45
40	831.27
50	1039.1
100	2078.16

Table 9 gives the borehole depth and resulting storage volume for the different cases. The storage volume is calculated from Equation 15. The volume increases with larger depths while all the other parameters where kept constant. The thermal conductivity, given Table 3, was assumed to be constant throughout the ground.

Table 10: Ratio between the collector area and the boreholes volume

Borehole volume	Collector area	Collector area/borehole volume
415.63	200	0.48
623.45	200	0.32
831.27	200	0.24
1039.1	200	0.19
2078.16	200	0.096

The amount of energy stored in the ground storage is increased with a larger storage volume. The heat losses on the other side will also be increased when the storage volume is made larger. From Equation 7 we can see that the solar collector efficiency increases with an increasing storage depth. Larger volumes give lower storage temperatures and the rest urn temperature to the solar collector will decrease. Lower inlet temperature to the solar collector efficiency will raise the efficiency. This since lower storage temperature will limit the collector temperature and thus the heat losses to the surroundings, expresses by Equation 16.

$$Q = UA(T_c - T_{amb})$$

Equation 16: Heat losses to the surrounding

Figure 23 and Figure 24 represents the storage temperature over the storage season for the different storage depths. The storage end temperature increases with a decrease in the storage depth. The end temperature in the storage after the storage season should be around 40°C so it can be used for direct heat exchange. The storage parameters and solar collector size are based on providing a relatively high storage end temperature

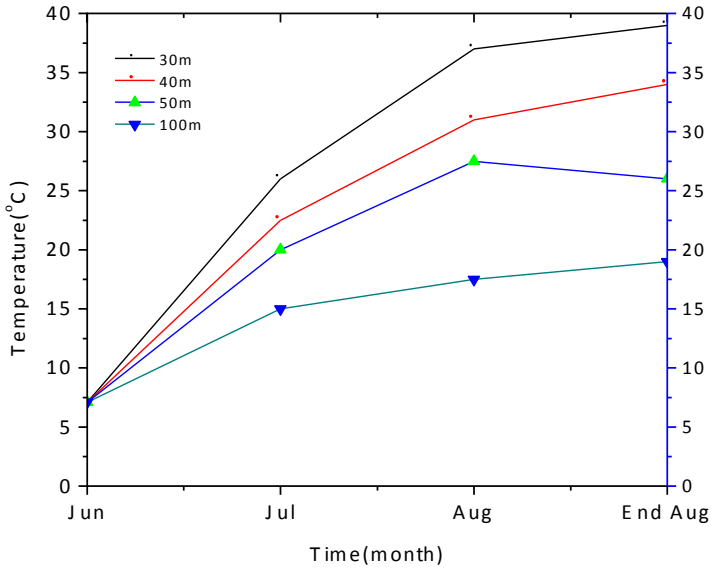

Figure 23: Storage Temperature with varied depth over the storage season

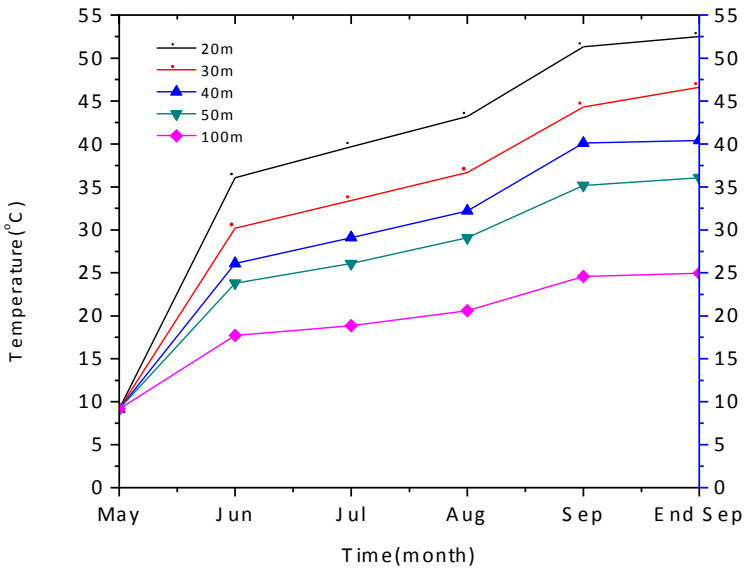

Figure 24: Storage end temperature for different borehole depths in Siping, China

The storage end temperature with varied borehole depth is shown in Table 11. As previously discussed it is favorable to have a storage end temperature around 40°C. Figure 23 and Figure 24 show that the temperature increases when the storage depth decreases. The storage depth is varied from 10m to 100m and the storage end temperature is at its highest when the borehole depth equals 10m. The graph shows the same changing tendency as for Trondheim and Siping but different values. Siping has a higher initial ground temperature and higher ambient temperatures in the summer month giving a longer storage season. Consequently Trondheim achieves a lower storage temperature but they both reach the demand directly supplying the load in the second heating mode.

Table 11:Varied depth and storage end temperature

Depth [m]	Trondheim [°C]	Siping [°C]
20.0	38.6	42.0
30.0	33.1	36.0
40.0	29.2	31.04
50.0	26.3	29.1
100.0	18.8	21.8

When the volume of the storage decreases the storage temperature will increase. Smaller volumes will give higher temperature in the ground and also higher return temperature to the tank. It can be seen from Figure 25 that the tank losses increase with the borehole depth. This is due to the increase in return temperature. The temperature in the tank will increase with the increase in supplied temperature from the ground giving a higher temperature difference between the tank and the surrounding. Equation 17 expresses the relations between the temperature difference and the tank loss.

$$Q_{tank\_loss} = \sum_{i=1}^{N} UA(T_i - T_{amb})$$

Equation 17: Tank losses

Decreased storage depths will increase the storage losses to the surrounding ground, Figure 25 and Figure 26. The initial storage temperature is the undisturbed ground temperature at the given location. For Trondheim this is 7.1°C and for Siping it's a bit higher at 9.17°C. Figure 25 and Figure 26 also shows that the amount of injected heat to the storage increases with the

storage depth. The injection of heat to the storage increases and lifts the storage temperature. The ground storage will then achieve a storage temperature larger than the initial temperature. This results in an increasing temperature difference between the storage and the surrounding ground. From Equation 14 it is seen that the heat losses increase when the temperature in the ground increases.

Figure 25 and Figure 26 provides some differences between Trondheim and Siping. Trondheim shows a higher value for the energy losses and gains. The trend is observed to be the same when increasing the storage depth as explained above. However, Siping experiences at a depth of 10m that the amount of storage losses is higher than the amount of energy stored.

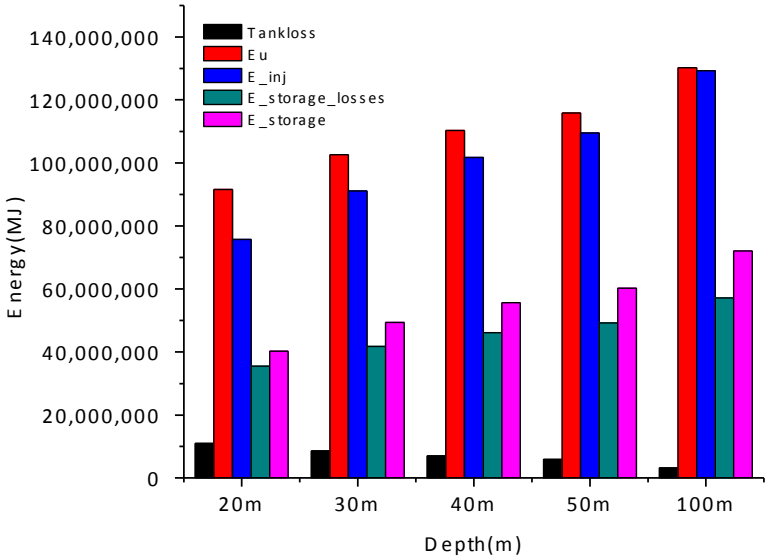

Figure 25: Energy loss and gain for different borehole depth in Trondheim.

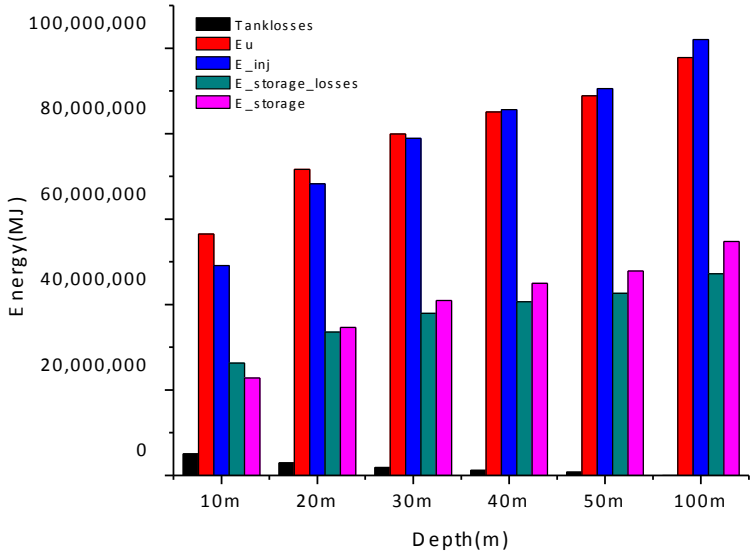

Figure 26: Energy loss and gain for different borehole depth in Siping.

The storage heat losses can be divided into tree parts, top losses, side losses and bottom losses expresses in Figure 25 and Figure 26. The total losses will increase with the storage depth and the side losses are the most dominant. This since an increase in borehole depth gives a larger heat transfer to the surrounding ground. The increase in top and bottom area does not increase in the same facto as the sides and actually decrease with increasing depth. It is seen that the side and top losses are almost non-existing when the storage depth is set to be 100m, this since the storage temperature decreases. All the losses added together show that the total storage loss increases with a larger storage volume, but on the other hand the storage efficiency is better for larger storages because the amount of useful energy gain is bigger.

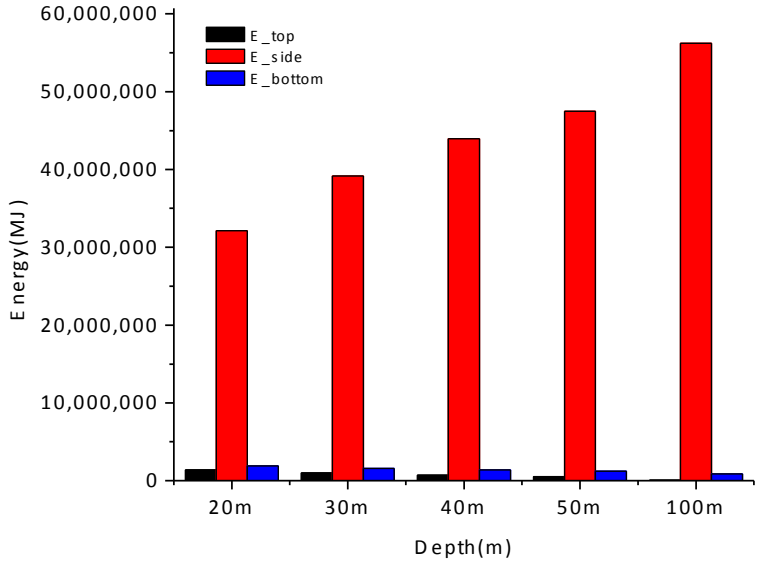

Figure 27: Storage losses for different borehole depth in Trondheim, Norway

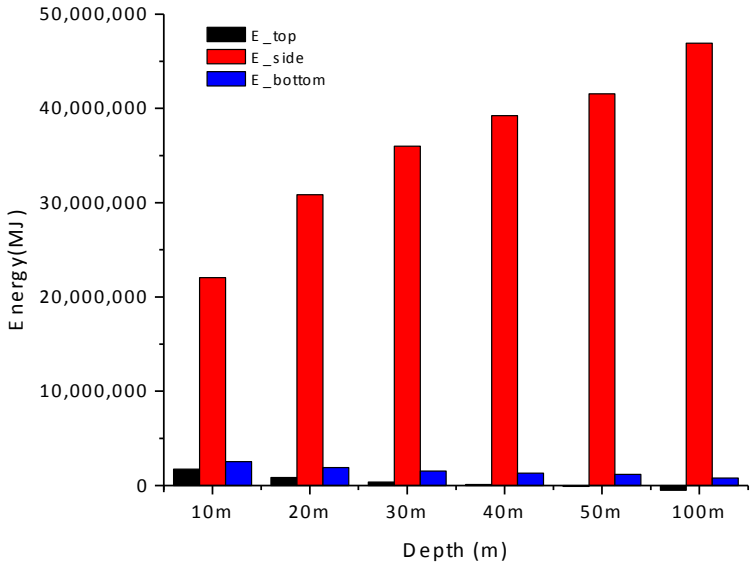

Figure 28: Storage losses for different borehole depth in Siping, China

The losses for Trondheim are higher than for the system in Siping. The ambient temperature and the undisturbed ground temperature are as previously discussed lower for Trondheim. This results in higher losses to the surrounding ground.

6.3.4. Optimization of number of boreholes and spacing

The spacing between the boreholes in the ground storage is an important parameter and need to be optimized. The storage volume is kept constant at 623.45m^3, while the borehole spacing is varied. When changing the spacing the number of boreholes changes according to Equation 15. Simulations were done for a spacing varying from 0.5 m to 3.5 m displayed in Table 12.

Table 12: Borehole spacing and number of boreholes

Spacing [m]	Number of boreholes
0.5	96
1	24
1.5	10
2	6
2.5	4
3	3
3.5	2

When the spacing between the boreholes are set to be small the storage temperature are high, this for spacing smaller than 1.5 meters. When the storage temperature is high the storage losses increase since the temperature difference between the storage and the surrounding ground increase, Equation 14. The storage losses will then be higher than the amount of stored energy. Larger spacing gives a smaller number of boreholes and thus the heat transfer area will reduce and the heat transfer will be smaller. This gives a lower storage temperature and then smaller storage losses to the ground.

The aim in the storage period is to store heat in the ground storage. For a seasonal storage the borehole storage will consist of several boreholes. The boreholes should be placed in compact patterns with small spacing since interactions between the boreholes are favorable. Figure 29 and Figure 30 show energy gains and losses with varied spacing.

Figure 29 represents the storage located in Trondheim. In Trondheim a spacing of 1.5m, resulting in 11 boreholes, is the best configuration. When the spacing is set to 1.5m the amount of stored heat and the amount of losses are almost equal but it is here the amount of stored heat is at its peak. For spacing smaller than 1.5m the amount of storage losses are higher than the amount of heat stored in the storage. For larger spacing the amount of stored heat will decrease. The amount of useful solar energy gain increases with decreasing spacing while the amount of tank losses have a limited increase with increasing spacing.

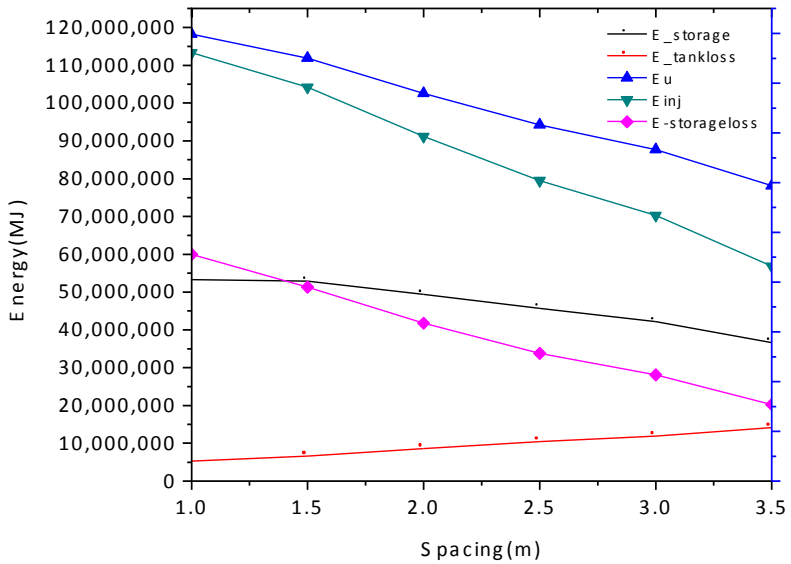

Figure 29: Optimizing the boreholes spacing, energy flows in the ground storage during storage season for Trondheim.

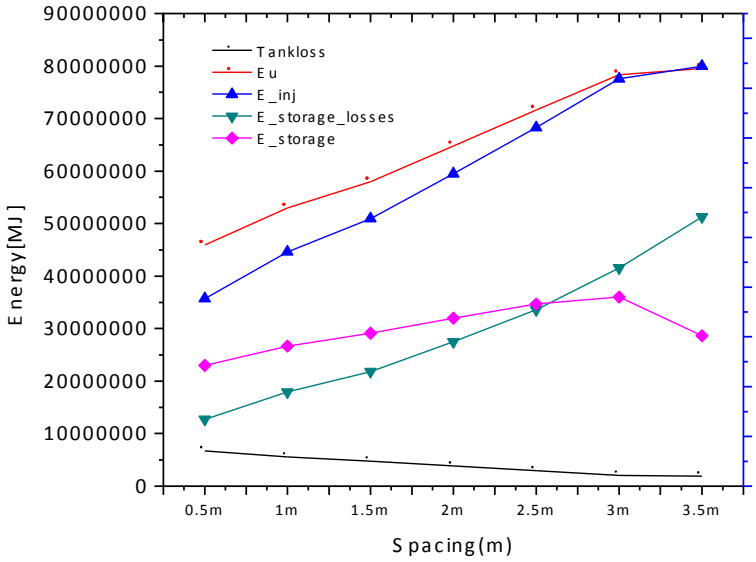

Figure 30: Optimizing the boreholes spacing, energy flows in the ground storage during storage season for Siping

The storage with different boreholes spacing located in Siping is given in Figure 29. The optimal spacing is found to be 2.5m. When the spacing is set to 2.5m the amount of stored heat and the amount of losses are almost equal but it is here the amount of stored heat is at its peak. From Table 12 this gives a total number of 4 boreholes. Figure 29 and Figure 30 displays how the spacing influences the storage system. When the spacing between the boreholes are set to be larger he storage temperature are high, for spacing larger than 3m the storage end temperature exceeds 40^{o}C. This is the opposite tendency compared to Norway. When the storage temperature is high the storage losses increase since the temperature difference between the storage and the surrounding ground increase, Equation 14. The storage losses become larger than the amount of stored energy when the spacing exceeds 2.5m. When the spacing is 2.5m the amount of stored energy is at its peak.

Table 13: Design parameters for the ground storage for Trondheim and Siping

Parameter	Trondheim	Siping
Borehole depth [m]	30	30
Borehole spacing [m]	1.5	2.5
Number of borehole [-]	11	4
Storage volume [m^3]	623.45	623.45

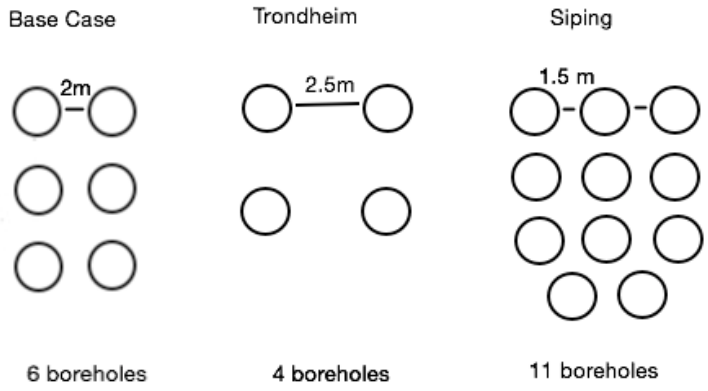

Figure 31: Borehole design for the Base Case, Trondheim and Siping.

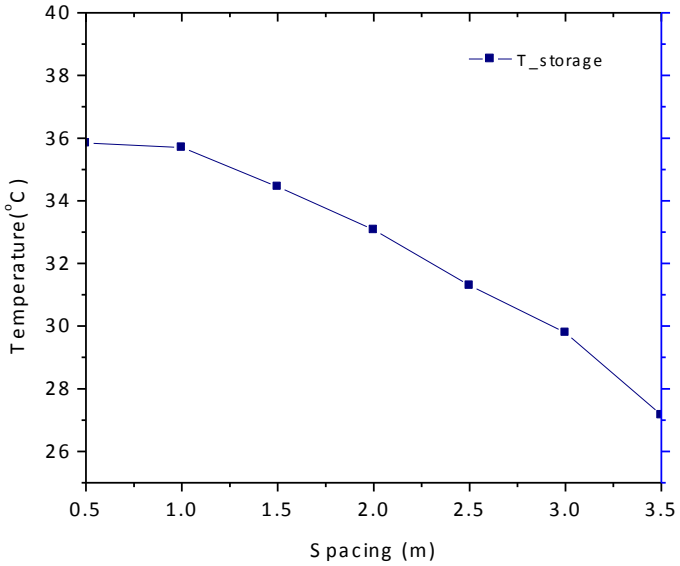

Figure 32: Storage temperature with different boreholes spacing during the storage season for Trondheim.

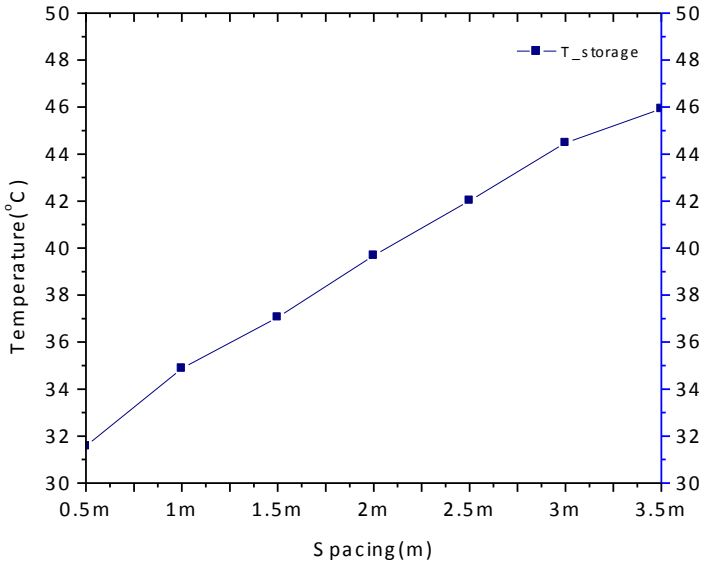

Figure 33: Storage temperature with different boreholes spacing during the storage season for Siping.

The parameters presented in Table 13 and design shown in Figure 31 will be used throughout the rest of the simulations.

6.3.5. Tank volume

The water thank is in this system used as a buffer store. 75-125L for every square meter of evacuated tube solar collector area, with a solar collector area at 200m^2 the volume of the storage tank were initially set to 20m^3. The system where then simulated with a tank area varying from 5m^3 to 30 m^3 to see of this value can be optimized. The results are shown in Figure 34.

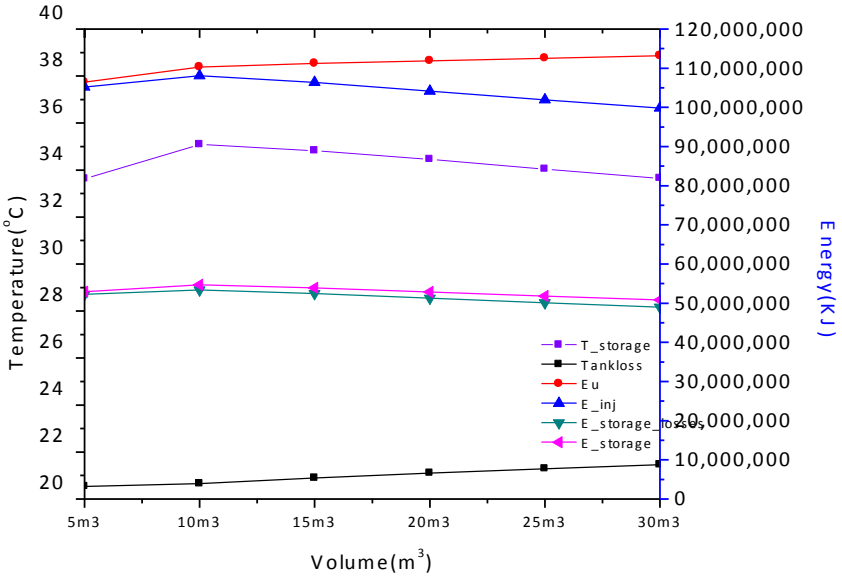

Figure 34: Storage temperature, energy gains and losses during the storage season with different tank volume, Trondheim

It is the tank losses and amount of solar gain that is mostly influenced by the tank volume. From Figure 34 it can be seen that the tank losses increase with a larger tank volume. The tank losses are the heat losses from the tank to the environment and expressed in Equation 17.

When the volume of the tank is increased the surface area increases thus the tank losses increase. The stratification is better for larger volumes due to better temperature. This will decrease the tank outlet temperature providing a lower inlet temperature to the solar collector. A lower inlet temperature results in better solar collector efficiency. Smaller volumes result in less stratification since there is less height to stratify the temperature. Then the solar collector efficiency will decrease due to higher inlet temperature provided by the tank. The storage losses and the storage temperature are not highly affected by the tank volume. The useful energy gain increases with larger tank due to the increasing solar collector efficiency for grater tank volumes

The optimal tank volume is in this case $10m^3$. At this size the amount of stored heat is at its maximum. The amount of stored energy increase until $10m^3$, when the volume increase form $10m^3$ the amount of stored energy starts to decrease. As the volume of the tank increases the heat losses in the tank also increase resulting in a decrease in the amount of energy going into

the ground storage. The volume increase results in a decrease in the stored energy in the ground due to increase in heat losses in the tank as the volume increase.

6.4. Simulation results of designing the solar ground storage model

6.4.1. Sizing the ground storage and the solar collector

The effect and impact of the ground storage size and the solar collector size was investigated as a part of the simulation. The heat losses from the ground storage depend on the size of the storage unit, the sizing, location and temperature during operation. If the storage has a large storage volume the amount of heat that can be stored is accordingly large, but the surface in contact with the surrounding ground will be larger. The storage heat losses are governed by the storage side losses, which will increase with increasing storage volume. Storage losses are highly dependent on the ground temperature, which in turn is dependent on the systems given location. Heat losses increases as the temperature different between the ground storage and the surrounding ground increases. The two locations investigated in this thesis, Siping and Trondheim, show how the heat are different due to placement. If the volume of the ground storage is decreased the storage temperature will increase. A higher storage temperature is encouraged but will result in higher heat losses. The optimal solution between heat losses and the storage temperature was investigated in the simulation of mode 1. It is seen that to compensate for the heat losses a ground storage system is good for larger scale. Summarized it is seen that the heat losses increased with increasing surface area and the amount of stored heat increases with increasing storage volume. To minimize the heat losses to the surroundings the ratio between the surface area and the storage volume should be kept as low as possible

Observing the trends of the solar collector it is seen that the size of the collector has a great impact on the system. Larger solar collector area will naturally absorb greater amounts if solar thermal energy. The return temperature to the solar collector will then be higher giving a lower efficiency. The solar collector efficiency depends on the return temperature. Less useful solar energy gain will result in less energy stored in the ground storage. This will in return give lower storage efficiency.

The intended usage of the system shapes the system design. The ground storage can be used to supply the whole heating season and minimize the use of auxiliary heating. In this case the

ground need to be kept at a high enough temperature and thus the solar collector area need to be large. This to increase the storage temperature as well as the storage volume is kept small. If the object is to use the keep the ground temperature at a suitable level for use with a heat pump by using the solar collector. Then the solar collector needs to be sized relatively small, this because the inlet temperature to the evaporator should not be too high. The ground storage needs to be large so it's possible to achieve lower storage temperatures. The volume of the storage tank needs to be small.

6.4.2. The affect of the storage temperature and heat capacity

For our system the objective is to use the ground for direct heat exchange. To directly use the water in the heating coil the ground temperature need to be higher than 30^{o}C. The storage volume should therefore be small in relation to the solar collector area. The ground storage temperature has a decreasing tendency and when the storage temperature reaches a certain level the heat pump can be set in operation. Larger storage volumes can naturally store larger amount of heat as well as the relative heat losses are smaller. When it is desired to store a certain amount of heat the storage volume need to be build large enough to compensate for the heat losses to keep the storage temperature at a high enough level. To help raise the ground temperature the solar collector should have a large surface area. Designing a system with larger underground energy storage and a large solar collector would be ideal if we only considered the objective of the system. The space requirements and installation cost will make such a system economical unfeasible.

The storage capacity depends on the outlet storage temperature of a given storage with a certain volume and temperature. The capacity of the system increases when the temperature difference between the inlet and outlet temperature increases. It is therefore encouraging with low outlet temperature. When transferring as much heat as possible to the ground storage the temperature difference will increase. To optimize the heating system the heat transfer in the soil should be increased. The borehole design, placement, spacing and number for boreholes, affects the heat transfer between the soil and the heat carrier fluid. The outlet temperature gives the minimum discharge temperature and the lowest temperature level in the system. The storage temperature affects the heat capacity of the storage. High outlet temperatures will reduce the storage capacity and may occur if the storage is wrongly designed. The system efficiency will always be reduced of the temperature is too high; this since too high temperatures decreases the tank efficiency and the solar collector efficiency.

6.4.3. Designing the BTES

When extracting heat from the ground storage it is favorable with large spacing between the boreholes to avoid interaction between them. In this system one purpose is to store thermal energy during the summer for use during the winter. Interaction between the boreholes is therefore desirable and a compact pattern with low spacing will be suitable for this application.

Initially as a springboard for the simulation the system consisted of 6 vertical boreholes, 3 in series and with a spacing of 2.5m. The storage depth was set to 30m while the header depth was 1.5 m. The storage volume was calculated to be 623.45 m^2 and kept constant. Simulation of the ground storage resulted in alteration based on the simulation results. The storage end temperature decreases with the storage depth due to larger storage side losses, even though the amount of useful energy gain and energy injected to the storage increases with higher depts. Looking at the heat losses to the surrounding ground it is seen that the storage side losses are the govern loss and by increasing the depth this loss will increase. The depth was kept at 30m, when this depth provides the highest amount of stored heat. The water storage tank was found to be $10m^3$ compared to its initial size of $20m^3$.

6.5. Storage mode – simulation of the operation condition

To investigate the operation conditions for the storage month simulations are done for different operation time in Trondheim to look at the effect. The storage months are varied to find the optimal storage period where the largest amount of heat can be stored in the ground. The storage months have initially been set to last from June to August, where the buildings heat demand is low or not present. The electricity consumption needed by the pumps in the system is important values when investigating the effectiveness of the system. Two loops are represented in the system, each having one pump. The first loop is the solar collector loop where we have a pump circulating the working media through the solar collector and the tank. The second loop is the ground storage loop where the pump circulates the working media through the BTES and the tank for heat exchange. The objective is to find the storage period that gives provides the storage with most heat avoiding too much electricity consumption by the pumps.

The values of important are the storage end temperature, heat losses and gains for the heat storage and the electricity consumption of the pumps.

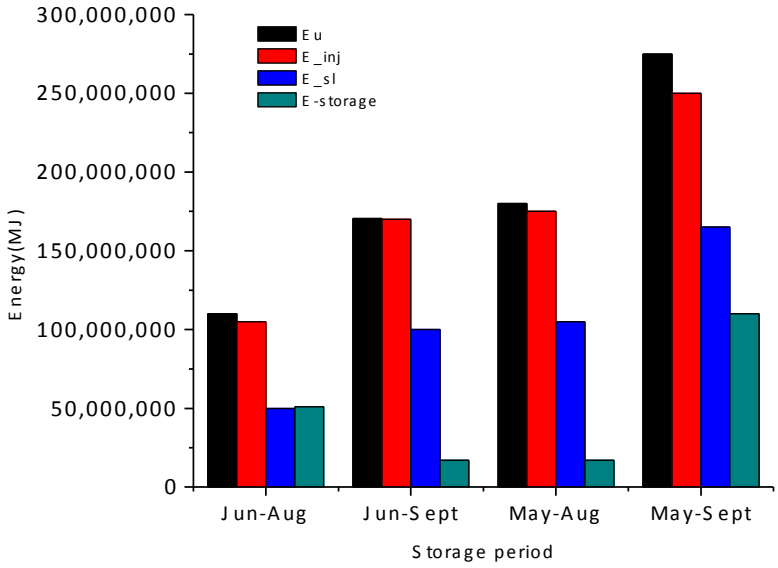

Figure 35: Heat loss and gains for different storage periods, Trondheim

The amount of useful energy, E_u and the energy injected to the ground storage E_{inj} has the same changing tendency seen from Figure 35. E_u and E_{inj} both increase with longer storage period and there are small differences between the two values. The tank losses stand for the difference in these values and the changes in the tank loss are small for changes in the storage period.

Figure 35 also show that the amount of heat stored into the ground storage increases with increasing storage period. The amount of storage losses also increases with the duration of the storage period. When the storage period is set too long the amount of storage losses becomes larger than the amount of stored heat. Since the storage losses are affected by the duration the amount of injected heat is larger than the amount of heat actually stored in the ground. When the storage period is short almost all of the heat injected to the ground storage is stored since the storage losses decrease.

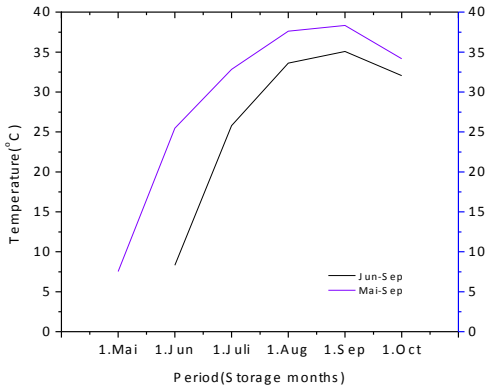

Figure 36: September as starting month

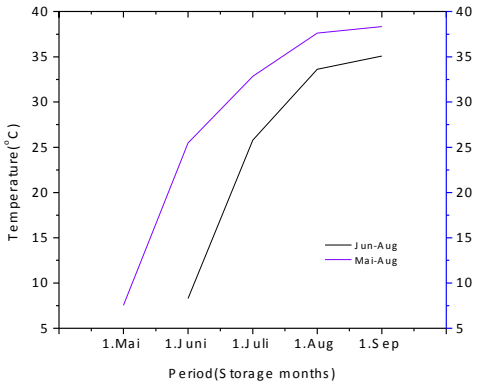

Figure 37: August the starting month

The storage length and the storage months affect the storage end temperature. The end temperature needs to be higher than 30°C to be used for direct heating. A higher end temperature result in a longer period of direct heating and the storage can provide more heat. With more direct heating the operation time of the pumps are decreases and consequently the electricity consumption.

Figure 36 and Figure 37 portrait how the storage temperature varies with the storage months. When the storage period is set to end in September it can be seen that the storage temperature decrease at the end. The temperature in Norway is low in September are resulting in larger heat losses in the storage and derby decrease in storage temperature towards the end. When the end month is set to August the temperature is sufficient higher. The start month resulting in the highest end temperature is May, and if we only look at the temperature the storage period should be set from May to August.

For a shorter storage period the electricity used by the two pumps decreases as the operation time is shorter. The electricity use is highest when the storage period is from May to Sep and smallest for a storage period from June to August. The start and end month of the storage period does not influence the electricity usage greatly. The electricity used by the solar collector pump from May to August and June to Sept is the same. There are small differences in the electricity used by the BTES pump when the month's change, but duration is the same. The operation time of the solar collector pump depend on the solar radiation because of the controller. By looking at the electricity usage the period that uses the least electricity is the shortest period, the storage period from June to August.

The compare the systems performance the COP for the storage are calculated for the different storage periods. The COP is the ratio between the amount of energy stored in the ground storage and the total amount of electricity used during the operation time. As described the system consist of two pumps, El_{SC} and $El_{BTES,}$ which stand for the electricity used. Equation 15 gives the COP for the ground storage.

$$COP_{storage} = \frac{E_{storage}}{El_{SC} + El_{BTES}}$$

Equation 15: COP for the ground storage

E_{store} The amount of energy stored into the ground storage [kJ]

El_{sc} Electricity use for the circulation pup in the solar collector loop [kJ]

El_{BTES} Electricity use for the circulation pump in the BTES loop [kJ]

If the COP for the storage is greater than one it implies that the amount of useful energy delivered to the ground storage is greater than the amount of electricity used. Table 14 shows the ground storage COP for the different storage periods. The COP is best for June to August, where the electricity uses are small due to short operation time. Calculations are found in Appendix G.

Table 14: COP for the ground storage

Storage period [months]	COP	24h
Jun-Aug	16.04	26.17
Jun-Sep	14.58	
Mai-Aug	14.14	
Mai-Sep	16.19	

A storage period from June to August is chosen for this system. The storage end temperature is highest for a storage period starting in May, but in this period the electricity consumption is higher giving a lower COP as well as higher storage losses. The storage period from June to August gives the second highest end temperature and the largest COP. The storage end

temperature is sufficient high enough with June as the starting month for direct heating (<30°C).

6.6. Simulation and results of operation mode 1

In the previous section different parameters has been varied and the storage mode simulated to determine the best values for this system. The evacuated tube solar collector has a collector area of 200m^2.The ground storage consists of 11 boreholes with a spacing of 1.5m while for Siping the optimal system design consist of 4 boreholes spaced 2.5m. The design parameters for Trondheim and Siping are presented in Table 15.

Table 15: Design parameters for Trondheim and Siping after simulation of operation mode 1.

Design parameter	Trondheim	Siping
Solar collector area [m^2]	200	200
Borehole depth [m]	30	30
Borehole spacing [m]	1.5	2.5
Number of boreholes [-]	11	4
Storage volume [m^3]	623.45	623.45
Tank volume [m^3]	10	10
Storage season [months]	May - September	April – October
Heating season [months]	October – April	November -Mars

Simulations for different parameters have been done to analyze and evaluate the operation of the storage model. The design parameters of the solar collector and the boreholes have been chosen with respect to the gains, losses and temperatures within the system. Weather conditions and radiation are dependent on the location and the time of year. Trondheim and Siping are two cities located at different geographical places meaning that the outside parameters differ. It has been observed that their monthly variations over the duration of a year show the same changing tendency with cold ambient temperature in the winter and warmer temperature in the summer. The solar yearly radiation is quite different for the Trondheim and Siping as well as the undisturbed ground temperature. The difference in these values is important input parameters in TRNSYS and influences the system design and performance.

The heat demand from the concept house governs the time of the heating and storage season. The same house is used as a heating load for Trondheim and Siping, but the resulting heating demand is not equal due to their external parameters. The different storage period is playing an important role in the temperatures, electricity use as well as energy gains and energy losses. The longer the pump needs to be in operation the more electricity it will need. As the duration storage period increases the amount of stored energy will increase, the energy losses will increase as well meaning a balance need to be established. By changing the different parameters the behavior of the system can be analyses and the system planned. It was interesting to see how the storage was influenced thorough the planning and sizing for two different locations.

Figure 38 presents the amount of energy gains and losses during the storage season for Trondheim and Siping. It can be seen that the amount of solar radiation is greater for the system located in Siping compared to the system in Trondheim. The solar collector areas for the two systems are chosen to have a size of 200m^2. Since Siping has a higher yearly amount of solar radiation the amount of useful energy will be higher than for Trondheim. The amount of useful energy is not that much higher for Siping than for Trondheim compared to the radiation. This decrease in the case of Siping is due to the heat losses to the ambient. The high temperatures created by the amount of radiation will create a larger temperature difference compared to the ambient temperature. The difference between the amounts of stored energy does consequently not differ that much between Siping and Trondheim.

Both Trondheim and Siping has ground storage with a volume of 623.45 m^3. They have the same depth of 30m but not the same number of boreholes or spacing size. Trondheim has a storage comprised of 11 borehole placed 1.5m apart. Siping has a storage consisting of only 4 boreholes with a spacing of 2.5m. After deciding the key parameters in the each system the storage end temperature need to be sufficiently high. The end temperature in the storage after the storage season should be around 40 $^{\circ}$C so it can be used for direct heat exchange. The storage end temperature for the two systems was found to be 41.59 $^{\circ}$C for Trondheim and 42.96 $^{\circ}$C for Siping. The storage parameters and solar collector size are based on providing a relatively high storage end temperature.

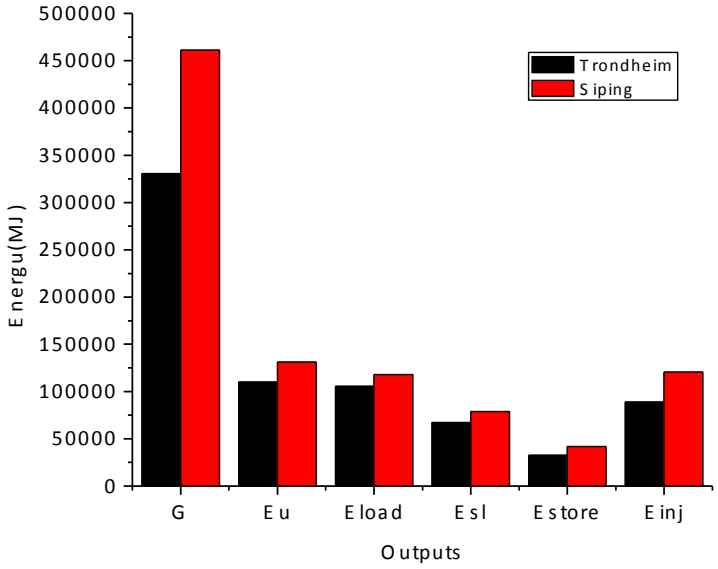

Figure 38: Energy gains and losses during the storage season for Trondheim and Siping during a typical year

It is favorable to have a compact pattern consisting of several boreholes when the intention is heat storage. This is to avoid heat exchange and heat losses between the boreholes. Both storages has a storage end temperature above 40°C even though their storage design is unlike.

Table 16: Storage temperature after the storage season

Storage end temperature [°C]	Location
41.59	Trondheim
42.96	Siping

Table 17: COP for the storage season for both locations, calculated from Equation 15.

Location	El_{SC} [MJ]	El_{BTES}[MJ]	E_{stored}[MJ]	COP
Trondheim	1124.44	5926.27	32437.5	16.02
Siping	1363.52	9858.33	41724.9	11.5

Siping does not need as many boreholes as Trondheim since the storage season is found to be longer and the ambient temperature during the storage season higher. Trondheim has a lower average ambient temperature and a lower undisturbed ground temperature resulting in a

storage design consisting of more boreholes. The amount of heat per meter tube length is 147.4MJ/m for Trondheim and 347.7MJ/m for Siping, the calculations can be found in Appendix G.

6.7. Simulation of the different heating modes

After designing the boreholes thermal storage and other system components the different heating modes needs to be investigated and simulated. Operation modes 2- 4 are as discussed in Section 3, all heating modes and are running during heating season. These three modes should all be set in operation in a prioritized order to achieve the best system performance. The heating modes should be run in the following order:

Solar direct heating (Mode 2) → direct heat exchange with the ground (Mode 3)→geothermal heat pump (Mode 4)

The different simulation modes will be simulated separately and the aim is to study their heating performance. The concept house simulated in section 6.2 represents the heating load. In each of the different modes a fan coil is used to distribute heat into the residential building. The heated air stream from the fan coil is pushed into the building and the temperature is based on the outlet air conditions and the inlet fluid and air conditions. This is an iterative process performed by TRNSYS and the temperature of the buildings zone temperature will change during the operation time due to the heated air stream.

As the different modes are simulated separately it may give different result than if the modes where implemented in the same TRNSYS file. This would have given better dynamic and provided different return temperatures when the operations work together. Such a system would require a lot of control strategies such as valves and controller, and a deeper knowledge to the software. Separate simulation will still show how the heating performance of each mode functions and how much of the buildings heating load each can cover.

The building heating load and the space heating system are the same for all the heating modes. The heating sources differ in each case and are prioritized to achieve a low electricity use high efficiencies. The first heating mode, the solar direct heating mode, uses a solar collector as a heat source in combination with a water storage tank. The second heating mode

is the direct heat exchange, where the borehole storage provides the heating. Geothermal heat pump is the last of the heating modes and here the heat pumps are the heat source. The geothermal heat pump will extract heat from the borehole storage to reduce the electricity consumption.

In all the different operation modes different control strategies are implemented to enhance the system performance and control the heating source and heating sink. On the demand side, the concept house, a thermostat is used to control the indoor temperature. The set temperature is 21^{o}C, also the indoor requirement for Norway [22], and the dead-band is set to ±2^{o}C. This means that the indoor temperature can float between 19^{o}C and 23^{o}C. The aim is to see how long and well the system maintain the temperature limits during operation. As long as the set temperature is reached it is regarded as covering the heating demand.

The heating season was found to be different for Trondheim and Siping. For Trondheim the heating season is from September to May. For Siping the heating season was found to be from October to April. This is the operation periods for the heating modes. The end storage temperature, found by simulation of storage mode 1, is used as an input parameter for the heating season.

6.8. Simulation of operation mode 2

In the solar direct heating mode it can be seen from Figure 26 that the system consist of three loops. The first loop is the heat source loop, the red loop, where the solar collector transfers heat to the water tank. An ON/OFF controller controls the solar collector pump based on temperature control. The water tank exchanges heat with the blue loop and are connected to a fan coil. The fan coil is the link the heat load loop connected to the concept house. The fan coil heats the air circulating in the green loop increasing the heat inside the building. As seen from Figure 39 there is two pumps in operation in this mode, one connected to the solar collector loop and one connected to the liquid side of the fan coil.

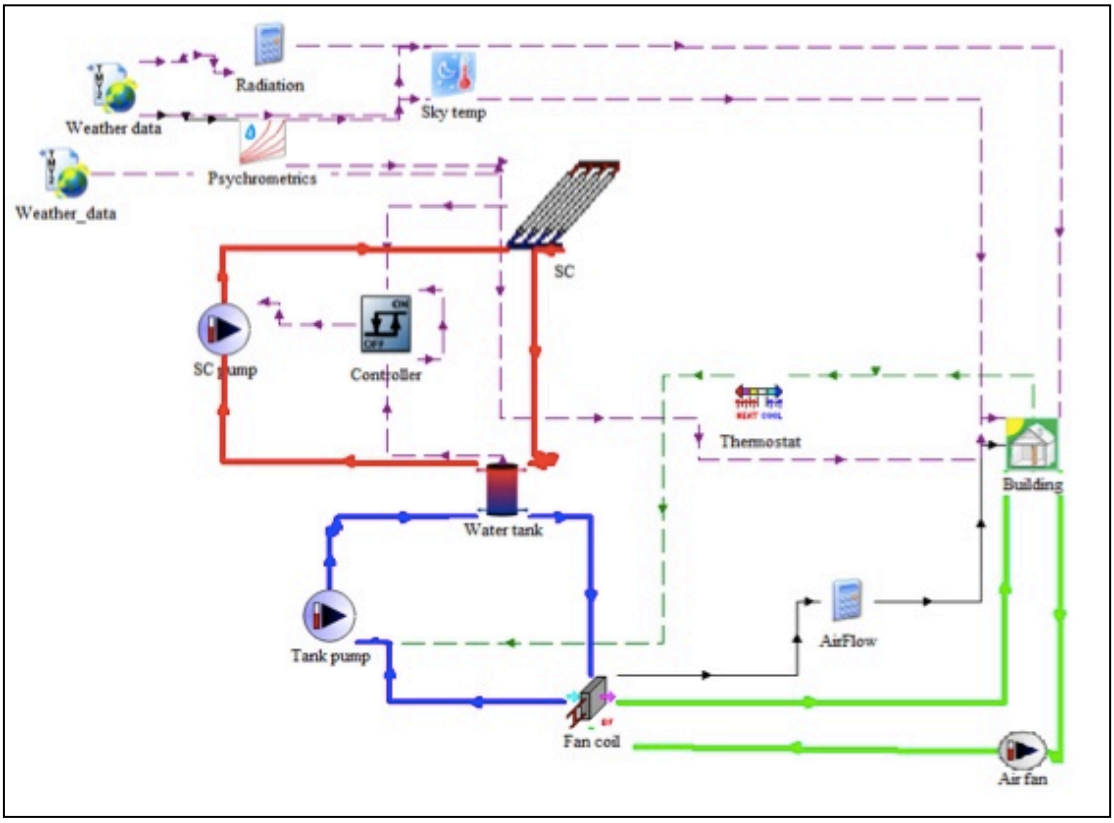

Figure 39: Simplified TRNSYS Sketch of operation mode 2, Solar direct heating

Table 18: Operation scheme heating mode 3

Operation mode	Solar Collector
2. Solar direct-heating In operation during heating season. The solar collector produces heat and the heat is exchanged in a solar water tank.	Produces heat at T>30^{o}C.

The objective of the simulation of the solar direct heating mode is to investigate how much of the heating load demanded by the house that can be covered by heat from the solar collector. The solar radiation and ambient temperature is the govern factor during this mode.

From Figure 40 and Figure 41 it can be observed how different temperatures vary and act throughout the entire heating season from Trondheim and Siping respectfully. The coverage is not good for the system located in Trondheim, but a larger part of the heating demand can be covered by direct heat for the solar collector located in Siping. For both locations the signal from the controller starts cycling ON/OFF when the collector outlet temperature goes too

high. This sine the thermostat is set to keep the room at the set temperature 21± 2°C. For Trondheim it can be found that the room temperature varies in a larger scale than for Siping. It is aspiration that the room temperature is kept around 21°C to ensure a comfortable indoor environment. For the system located in Trondheim it can be observed that the room temperature starts at a varying but high temperature level before falling down around the set temperature. When the operation time reaches the coldest winter months the temperature of the room decrease and fluctuates at a low temperature level. At this point the solar collector does not manage to supply enough heat to satisfy a comfortable environment inside the house. This is due to the poor amount of radiation Trondheim experiences during the winter months. The amount of heat obtained by the solar direct heating mode is highly dependent on the variation of the ambient temperature as well as the durational changes of the solar radiation. For Trondheim the temperature in the winter months are low. The solar radiation for January and February are almost not existing observed form Figure 13. As the ambient temperature and the solar radiation increases the heat from the solar collector increases and the room temperature is raised to approximately the set value.

The temperature behavior for the direct heating mode located in Siping show a more stable room temperature that is kept at a higher level. Figure 41 shows that the room temperature is kept high until the middle of the heating season when the ambient temperature reaches its minimum value as well as low solar radiation. Compared to Trondheim it can be seen from Figure 14 that Siping has an overall higher ambient temperature and a considerably higher solar radiation in the winter months.

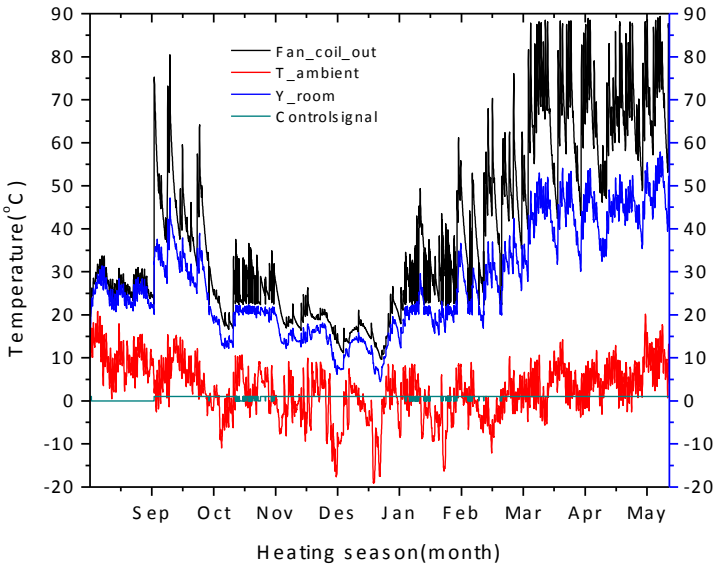

Figure 40: Simulation of Mode 2 over the entire heating season, Trondheim.

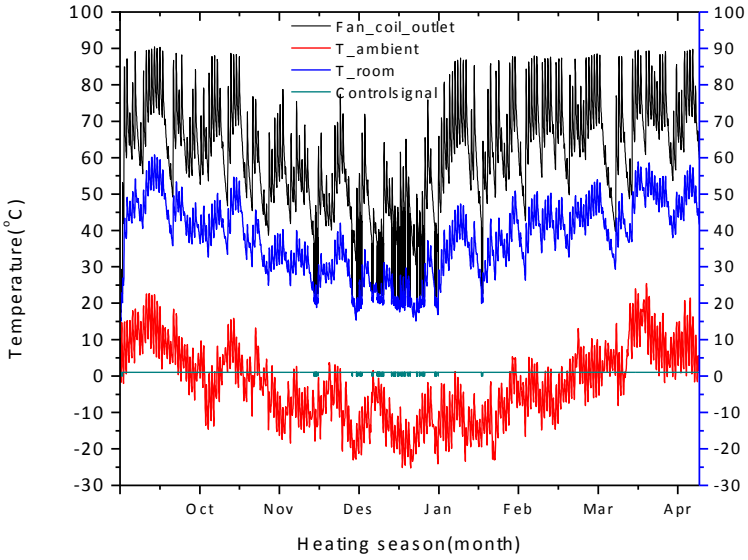

Figure 41: Simulation of Mode 2 over the entire heating season, Siping

The energy delivered from the heating coil and the heating demand is presented in Figure 42 and Figure 43. The house heating demand increases as the ambient temperature decrease. With a lover ambient temperature the temperature difference between the indoor and outdoor temperature increase. Consequently the house requires more heat to maintain a sufficient room temperature. In Trondheim the heat supplied from the heating coil falls in

December and January. This can be seen in comparison with Figure 40 where the room temperature and the collector outlet temperature decreases as the solar radiation in these months are considerably low. For Siping the energy supplied by the heating coil follows the shape of the heating demand. In both Figure 42 and Figure 43 the heating from the heating coil is below the heating demand of the building. For Siping the solar collector is able to supply sufficient with energy, while the limitations from the radiation leads to a low share of energy supplied from the heating coil in Trondheim

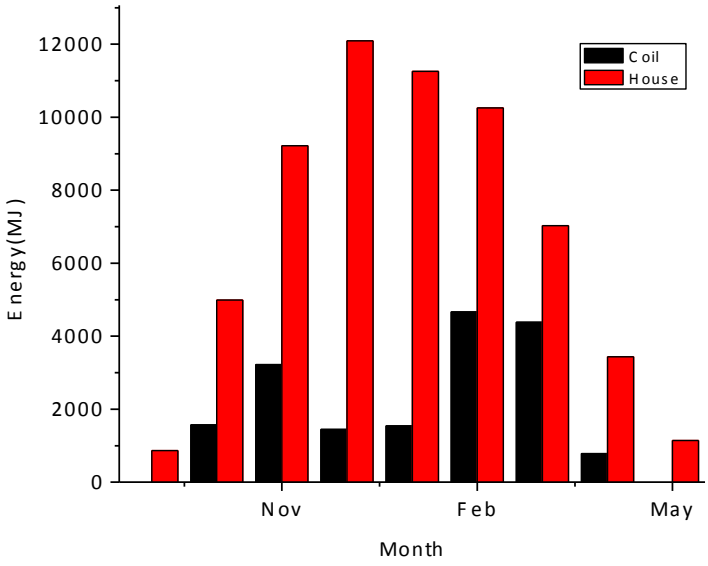

Figure 42: Energy supplied by the heating coil and the heating demand during the entire heating season, Trondheim

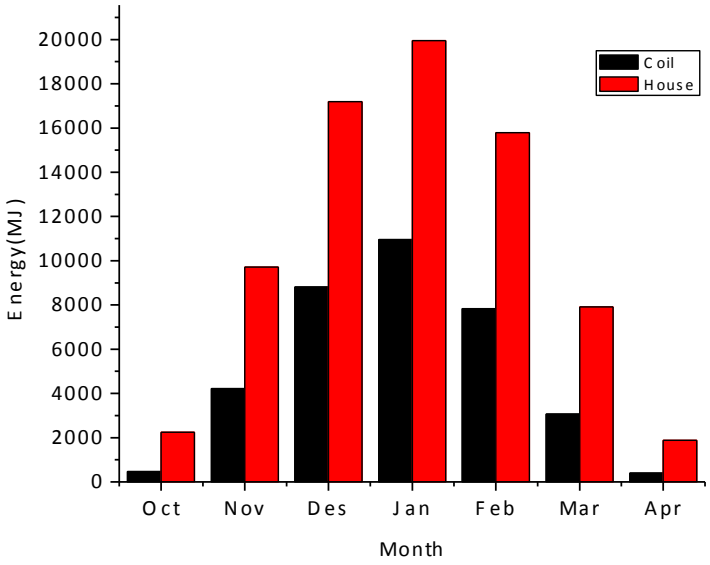

Figure 43: Energy supplied by the heating coil from the solar collector and the heating demand during the entire heating season, Siping.

Figure 45 show how the solar radiation and the solar fraction extend over the heating season for Trondheim and Siping respectfully. For both figures the solar radiation that hits the solar collector is showing a natural convex shape following the yearly ambient temperature variations. It can be observed that for Trondheim the solar radiation show a steeper decrease as the heating season is longer and the solar radiation is very low for the coldest months. Siping show a more stable solar radiation curve during the heating season. The solar radiation is present even in the coldest months. The solar fraction is a function of the heating demand and the heat supplied by the heating coil. The shape of the energy supplied from the heating coil, heat supplied from the solar collector, governs the shape of the solar fraction. For Siping this gives a concave shape since the amount deliver is considerably high compared to the heating demand of the single residence. The heat supplied from the heating coil in Trondheim is as discussed low for December and January while the heating demand is at it's highest. This gives low solar factor and a crack in the graph. The solar fraction is calculated according to Equation 2. The total solar faction for the entire heating season is calculated to be 0.29 for Trondheim and 0.65 for Siping. The solar factor for Siping is found to be very high. This can indicate that the sizing of the solar collector may be optimal but not realistic compared to the heating demand of a single residential building located in Siping.

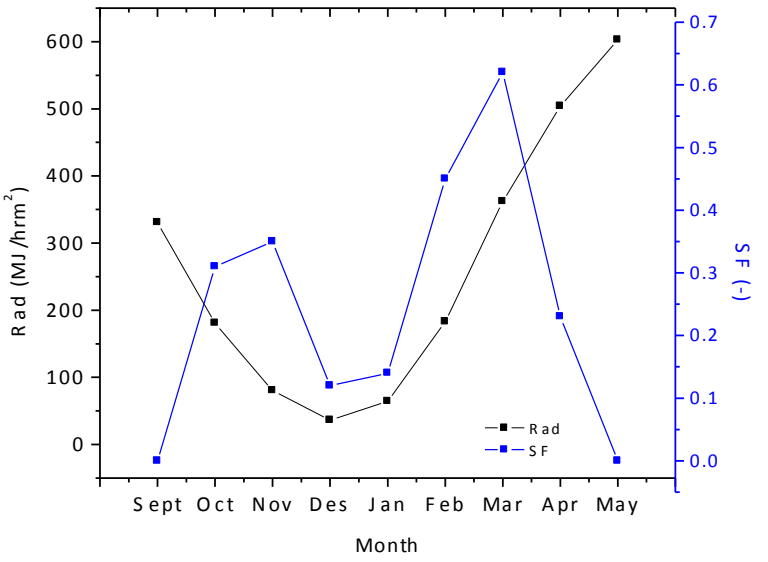

Figure 44: Solar radiation and solar fraction during the entire heating season, Trondheim.

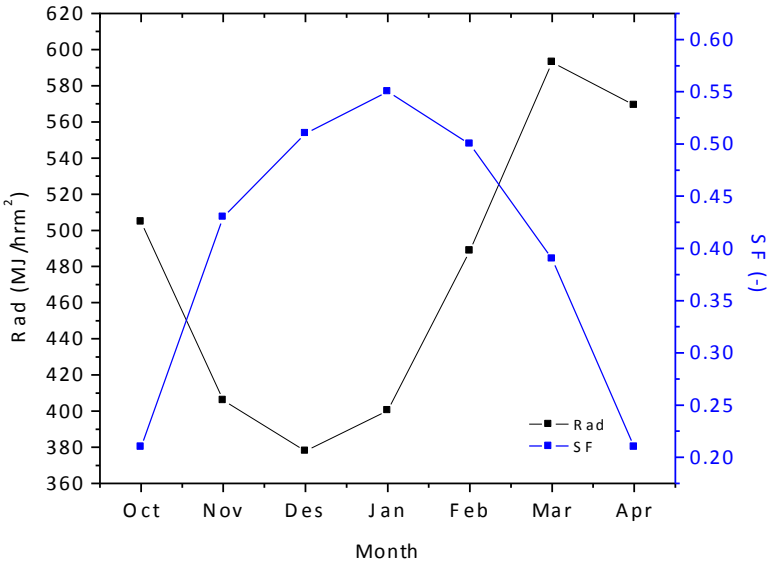

Figure 45: Solar radiation and solar fraction during the entire heating season, Siping.

6.9. Simulation of operation mode 3

Simulation mode 3 is the direct heat exchange with the ground. Figure 46 displays two loops. In the blue loop hot water is extracted from the borehole ground storage by a ground pump exchanging heat at the fan coil. The fan coil exchanges heat from the fluid inlet side to the air outlet side, supplying heat to the building. The circulation pump in the storage loop is the electricity user in this mode.

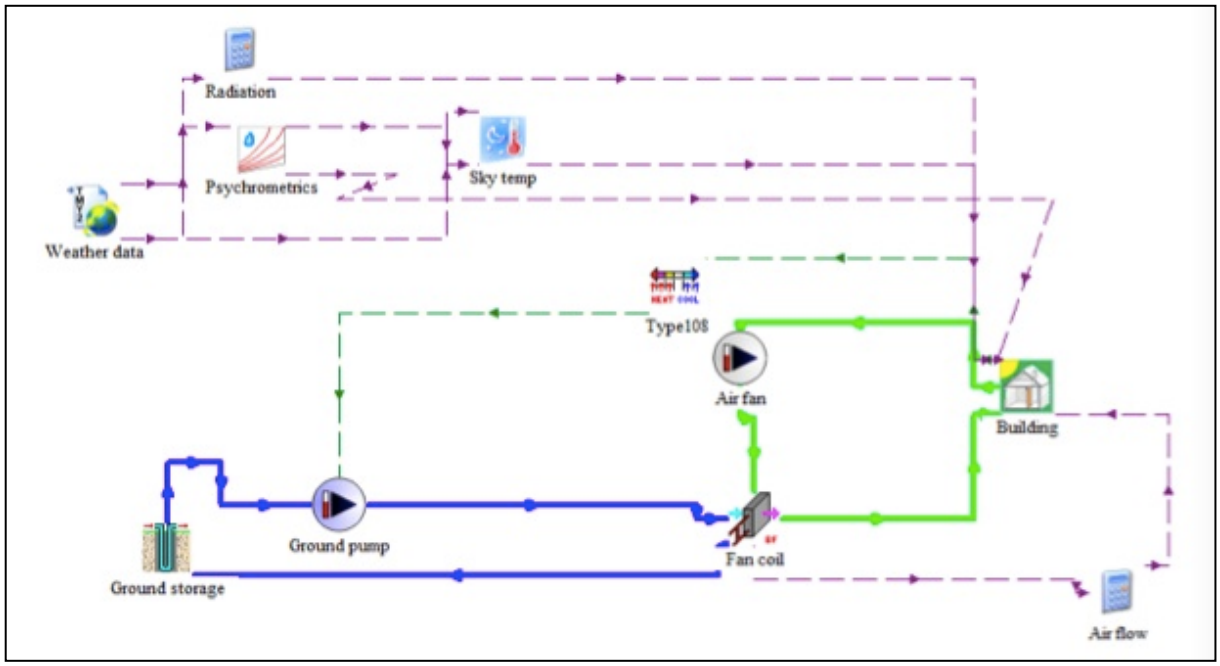

Figure 46: Simplified TRNSYS sketch of operation mode 3, direct het exchange with the ground

Table 19: Operation scheme heating mode 3

Operation mode	Borehole
3. Direct heat exchange with the ground In operation during heating season.	Heat is extracted and used to supply heat to the building. This for T>30^{o}C.

The parameters established after simulation of the storage mode is kept constant during this simulation. For the direct heat exchange with the ground the objective is to establish how much of the heating load that can be covered with heat extracted directly from the boreholes. The temperatures throughout the operation time for the system is look at to see how long the system can keep the room at the set temperature. After the simulation of Mode1 the storage

temperature was found to be 41.59°C and 42.96°C for Trondheim and Siping respectively. This is set as the initial temperature of the storage.

Figure 47 and Figure 48 show how the temperatures vary during the heating season for Trondheim and Siping respectfully. When the storage temperature drops to a certain level, around 30°C the heat distributed to the house is not plenty enough to keep the room temperature at the set level.

From Figure 47 it can be seen that the room temperature is no longer kept at 21°C when the storage temperature drops below 35°C. At this point the room temperature drops and are no longer kept stable this as the ambient temperature gets colder. The temperature keeps decreasing as heat is ejected from the storage and lost to the surroundings. As the ambient temperature increase at the end of the heating season the storage temperature increase as well, the temperature difference between the surrounding ground and the storage will decrease providing lower losses to the ambient. The room temperature is kept above the set limit when the ambient temperature increases.

When the temperature drops below 36°C, seen in Figure 48, the room temperature starts to fluctuate and the set temperature if the room is not satisfied. The storage temperature decreases rapidly explained by the quick decrease in the ambient temperature. The ambient temperature in Siping is kept at low levels most of the heating period resulting in a short period where the heat directly extracted from the boreholes manages to keep the room temperature high enough. The ambient temperature in Trondheim is more stable and does not reach as low temperatures as Siping. Storage losses to the ambient will then decrease and the storage temperature is kept at a higher level longer.

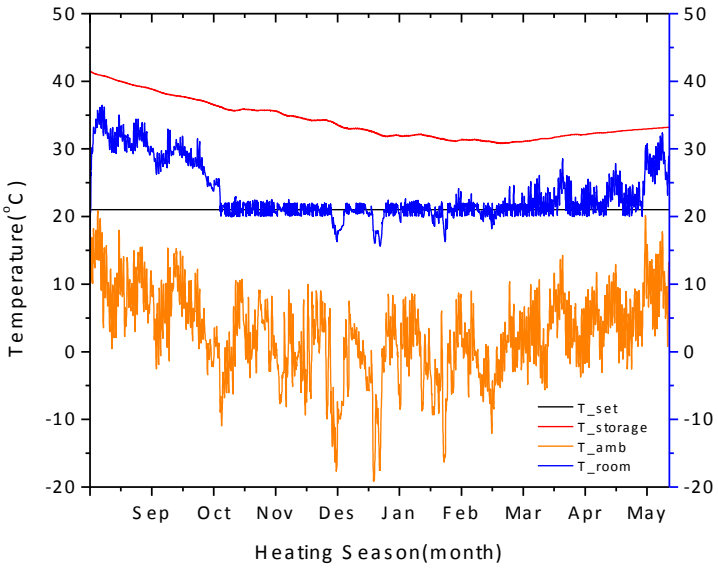

Figure 47: Temperature distribution during the entire heating season for direct heat exchange with the ground, Trondheim.

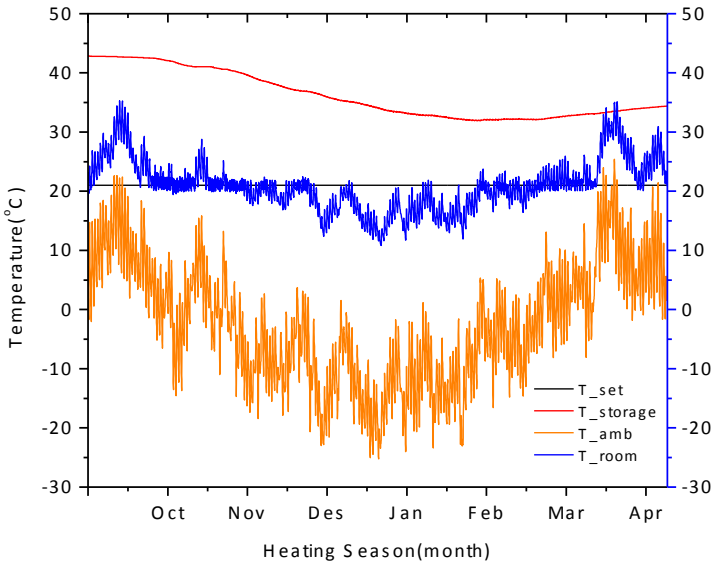

Figure 48: Temperature distribution during the entire heating season for direct heat exchange with the ground, Siping

6.10. Simulation of operation mode 4

The last heating mode put in operation is the geothermal heat pump. This mode consists of three loops illustrated in Figure 49. The red loop transfers heat from the ground storage to the evaporator where the heat pump exchanges heat with the liquid in the blue loop. The liquid side of the fan coil transfers the heat to the air stream circulating through the building in the green loop.

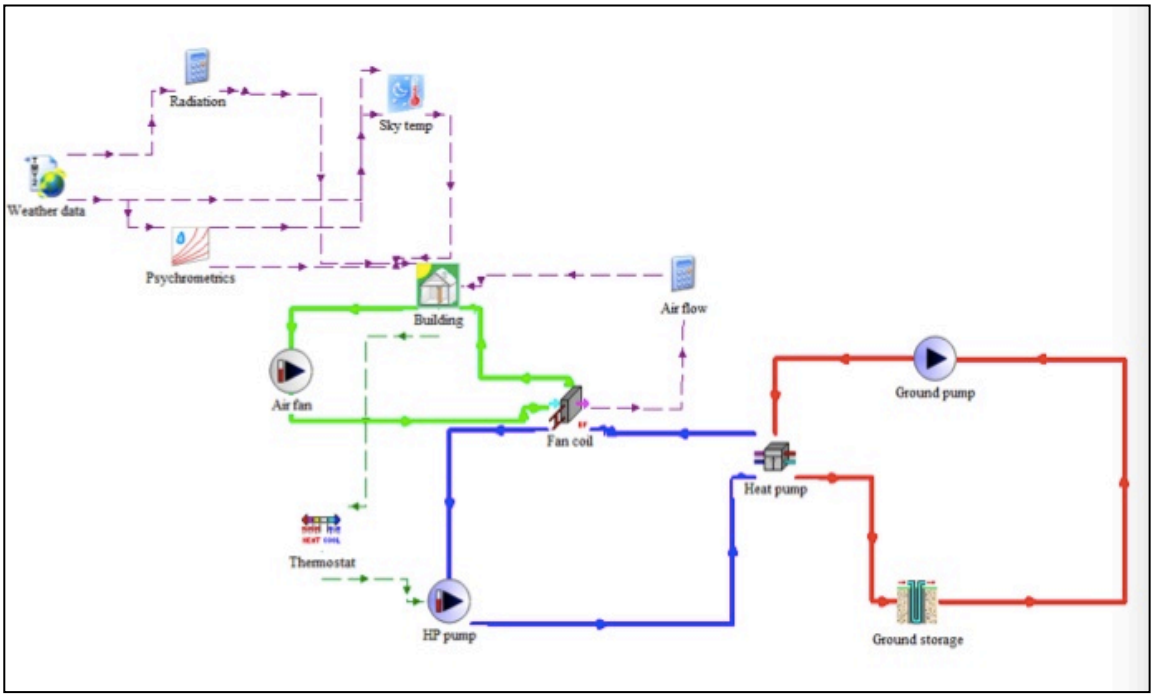

Figure 49: Simplified TRNSYS sketch of operation mode 4, geothermal heat pump

Table 20: Operation scheme heating mode 4

Operation mode	Borehole	Heat Pump
4. Geothermal heat pump In operation during heating season. When the boreholes don't have sufficiently high temperature for direct heat exchange. The heat pump provides heating while the boreholes are used as a heat source for the pump.	Heat is extracted from the boreholes.	For T<30°C the heat pump will start operating.

Figure 50 and Figure 51 illustrates the storage temperature, the inlet and the outlet temperature of the evaporator. The performance of the water-to-water heat pump used in this system is determined by the temperature of the water going in to the evaporator, in other words the temperature rise of the evaporator. In this case the COP will decrease with the inlet temperature of the evaporator, the temperature supplied by the ground storage. As seen from, the fluid temperature drops below 0°C during the simulation time. This fallout occurs since the ground temperature goes below the freezing point during the winter months. When the temperature of the working fluid drops below 0°C the system will perform inadequately, this since the water will freeze at temperatures below 0°C resulting in frozen boreholes. The temperature out of the storage and in to the heat pump will then be too low and this will be damaging for the heat pump. Because of the low storage depth and small storage volume the temperatures are unstable and at a low level. The ambient temperature and weather conditions will have a great impact on the storage temperature at too shallow depths.

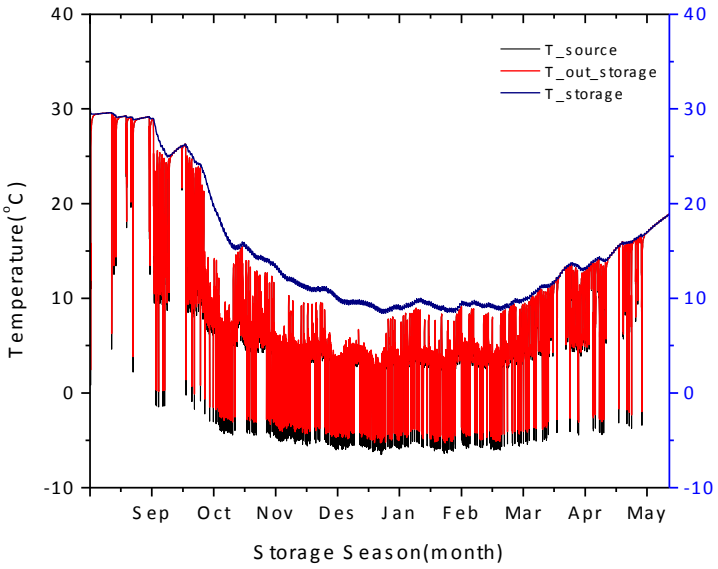

Figure 50: Temperatures during the entire heating season with a storage depth of 30m, Trondheim

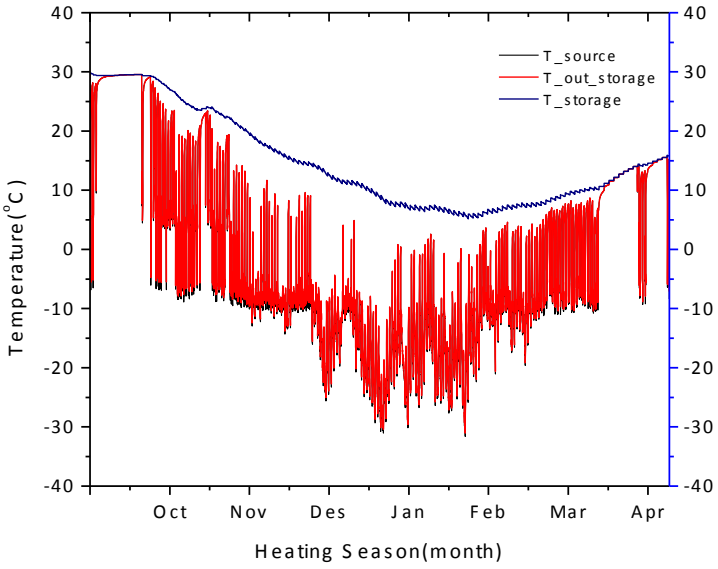

Figure 51: Temperatures during the entire heating season with a storage depth of 30m, Siping.

For both Trondheim and Siping the borehole depth is found to be too short. The borehole depths are found to short due to the low and unstable temperature shown in Figure 50 and Figure 51. To utilize the GHP in a resourceful way the storage temperature need to be higher and more sable. The depth is therefore increased in order to avoid too cold temperatures. The initial depth for both locations is 30m. For Trondheim the depth is increased to 150m while it is increased to 200m for Siping. The storage temperatures in Siping are lower in the winter months then for Trondheim and larger increase is necessary to increase the temperature.

From Equation 16, it is observed that the increase in the ground temperature during the summer is not balanced with the decreased in the winter. The heat transfer rate is higher in the winter than in the summer. As seen the temperature decrease in the heating season is stepper since the boreholes are designed too short and with a small volume.

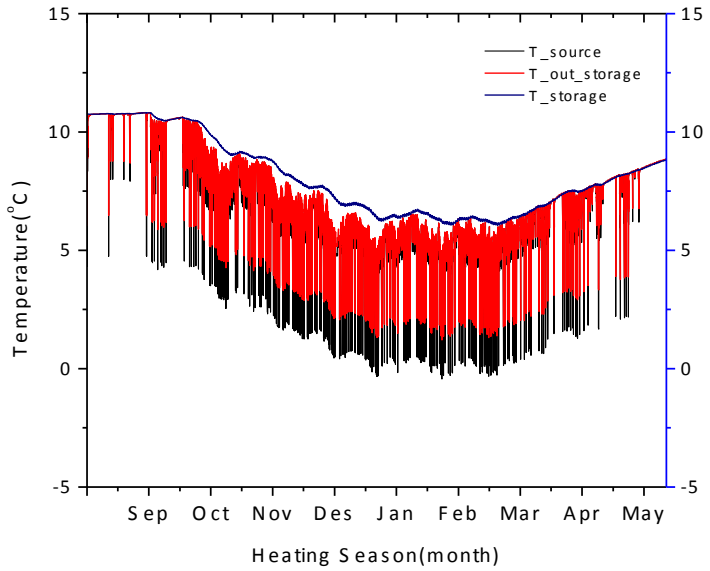

Figure 52: Temperatures during the entire heating season with a storage depth of 150m, Trondheim.

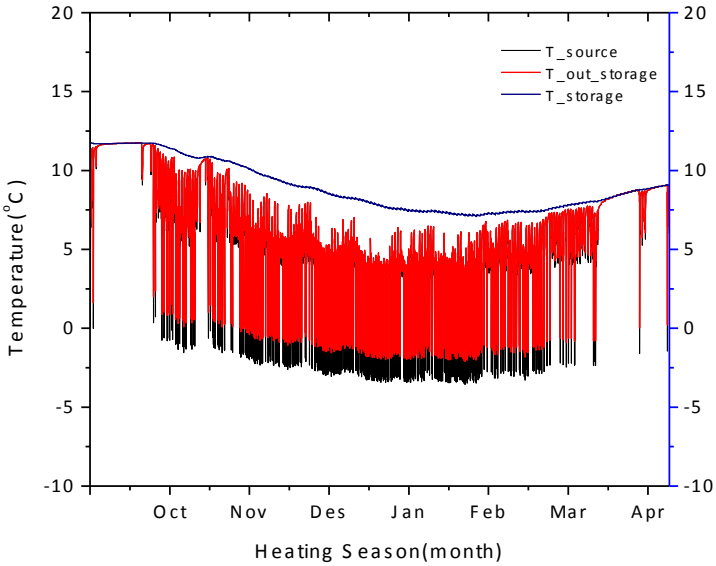

Figure 53: Temperatures during the entire heating season with a storage depth of 200m, Siping.

The new ground temperatures are calculated by steady-state calculations, see Appendix E.

$$\rho c_f V_1 (T_{30} - T_a) = \rho c_f V_2 (T_a - T_{18})$$

Equation 16: Ground temperature calculations

ρc_f Storage heating capacity of the soil [kJ/m^{3}K]

V_1 Volume in the base case of a borehole depth of 30m [m^3]

T_{30} The original storage temperature of 30˚C after operation mode 3 [℃]

V_2 New increase volume with the belonging new depth [m^3]

T_a Average temperature [℃]

T_g Average mean temperature of the soil [℃]

The new ground temperature was found to be 10.81˚C and 11.79˚C for Trondheim and Siping respectfully. The calculations of these temperatures are shown in Appendix E.
From Equation 16, it is observed that the increase in the ground temperature during the summer is not balanced with the decreased in the winter. The heat transfer rate is higher in the winter than in the summer. As seen the temperature decrease in the heating season is stepper since the boreholes are design too short and with a small volume.

Figure 52 and Figure 53 show the temperature after increasing the borehole depth. It can be observed that the temperatures become more stable and that the inlet and outlet temperature of the evaporator have increased. With deeper boreholes seasonal variations and the ambient temperature, as discussed in section 2.6, less influence the grounds. At deeper depths the ground temperature is kept at a higher and more stable level throughout the heating season. The heat pump will only be put in operation when the other modes are unable to supply sufficient enough heat to cover the heating load.

The geothermal heat pump mode was also simulated for an unheated system, where the ground is not heated in advance. The initial temperature is then equal to the undisturbed ground temperature at the given location and the heat pump will receive less support from the ground compared to a heated storage. In our case the initial storage temperature is 7.1 ˚C and 9.17 ˚C for Trondheim and Siping respectfully. The COP for the heat pump with heated storage for the entire heating season was found to be 2.78 and 2.54 for Trondheim and Siping

respectfully. For an unheated storage the COP show a small decrease ending up at 2.63 for Trondheim and 2.48 for Siping. The temperature at the inlet of the evaporator is raised since the COP is higher for a heated storage. There are not great differences since the storage depth had to be increase to avoid freezing boreholes meaning that the temperature lift left after mode 3 is not exploited.

6.11. Results

Table 21 shows the heat supplied during the different modes running over the heating season and their coverage of the heating load. The geothermal heat pump mode is covering the highest par, with 52.9% of the heating load, for the system located in Trondheim. The direct heat exchange with the ground covers 27.9%, while the solar direct heating mode covers the lowest part accounting only for 19.2% of the load. For the system located in Siping the coverage is distributed differently among the operation modes. The main share of the heating demand is covered by the solar direct heating mode, with 47.5%. The direct heat exchange with the ground only accounts for 11.97% while the geothermal heat pump covers the remaining 40.53%.

Table 21: Heat supplied in the different modes use within the heating system

Operation mode	Trondheim		Siping	
	Supplied heat [MJ]	Percentage of the load	Supplied heat [MJ]	Percentage of the load
Mode 2	11747.67	19.2%	35485.98	47.5%
Mode 3	17072.38	27.90%	8938.07	11.97%
Mode 4	32372.14	52.9%	30265.78	40.53%

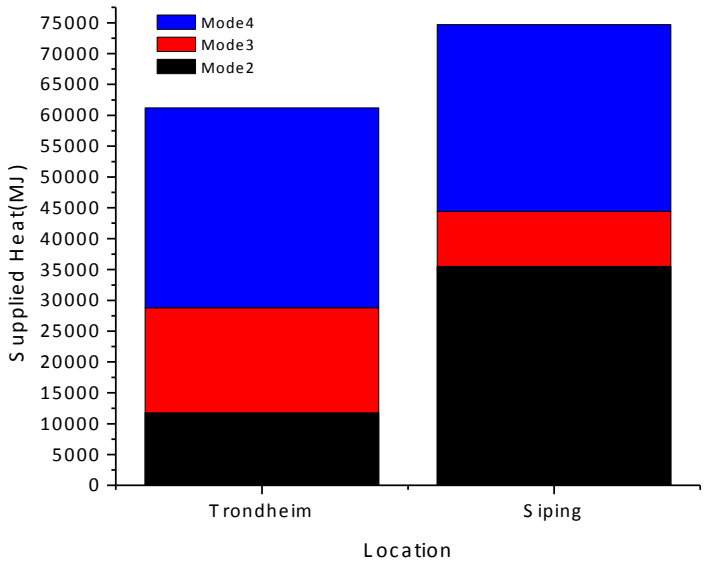

Figure 54: Amount of heat supplied in the different modes use in the heating modes for Trondheim and Siping.

Due to low solar radiation in Trondheim during the winter months the solar direct heating mode cannot cover large parts of the heating load. In Siping on the other hand the solar radiation is still high in the winter resulting in 47.5% coverage of the heating demand. The solar direct heating mode covers a larger part of the heating load for Siping also because the heating load of the house is lower, see section 6.2. In an optimal solution the area of the solar collector could be decreased for this system. Siping show an overall higher ambient temperature and a higher solar radiation. The direct heat exchange is the dominant source for neither Trondheim nor Siping. Both locations experience low temperatures in from December to March and room temperature is only kept at a high enough level a short period. From the weather data used in the simulation the, see section 4.4 Siping experiences lower peak temperatures and the direct heat exchange mode can only cover 11.97% of the heating demand. Trondheim has overall a bit higher temperature in the winter months and the direct heat exchange mode covers 27.9% of the heating load.

All the different modes had pumps circulating the medium and fans that required electricity to operate. The total electricity required for the entire system is summarized in Equation 17.

$$\sum E_{el} = E_{pe} + E_{pSC} + E_{pDX} + E_{HP} + E_{pHP}$$

Equation 17: Electricity use within the system

ΣE_{el} Total use of electricity within the system [MJ]

E_{ps} Electricity use of pumps operating during Mode 1 [MJ[

E_{pSC} Electricity use of pumps operating during Mode 2 [MJ]

E_{pDX} Electricity use of pumps operating during Mode 3 [MJ]

E_{HP} Electricity use of the heat pump operating during Mode 4 [MJ]

E_{pHP} Electricity use of pumps operating during Mode 4 [MJ]

Figure 55: Amount of electricity used for the different heating modes for Trondheim and Siping

Table 22: Results for operation of the different modes

	Electricity use [MJ]	
	Trondheim	Siping
Mode 1		
SC pump	1124.44	1363.52
BTES pump	5926.27	9858.33
Mode 2		
SC pump	331.97	1420.1
Tank pump	14.90	22.30
Mode 3		
BTES pump	1332.69	494.38
Mode 4		
Heat pump	1162.7	848.76
Source pump	104.0	28.2
Load pump	35.2	27.2
Sum	=10 032.1	=140 062.8
Unheated storage		
Heat pump	2175.35	4838.97
Source pump	196.56	152.64
Load pump	68.18	157.23
Sum	=2440.1	=5148.84

7. Conclusion

The scope of this research was to develop a model using the simulation software TRNSYS based on design parameters of a small town building located in Trondheim and Siping. The concept house is designed like a characteristic small residential house and has the same design for both locations. The system principles and operation modes used are the same for Trondheim and Siping but through optimization the resulting design was found to be different. The ambient temperature, ground temperature and the amount of radiation are different for the two locations. This results in different amount of heat demanded by the concept house, length of the storage/heating season and different design parameters for the different components.

During the simulation of the storage season the behavior of different parameter were investigated to obtain the optimal design. SAGSHP are environmentally friendly and therefore a good substitute to traditional space heating systems. Traditional geothermal heat pumps show stable operation efficiency when the temperature is kept stable at a decent level. This is achieved when the storage is constructed deep enough, around or below 10m, to avoid seasonal temperature variations. When the yearly natural charging and discharging of the ground is inadequate the ground temperature will decrease. This will give the heat pump poor operation conditions and the performance will decrease and a solar collector is used to avoid this trend. The solar collector is directly used for heating and charge the ground storage in the storage season in this combines system.

The results of the simulation of the storage season are presented in confirm that the size and design of the ground storage is of great importance. If was found that the performance of the system is closely linked to its size. The performance of the solar collector is dependent to the return temperature from the storage entering the collector. It is important that within the storage there is good heat transfer to ensure that solar collector inlet temperature is not too high. When the storage return temperature is kept low the solar collector efficiency will increase. For a large solar collector and a small storage volume the temperature will be high making it a system suitable for direct heating. When the storage volume is kept large and the solar collector area small the temperature will be lower making it suitable for the operation of a heat pump.

Simulation of the heating season for Trondheim and Siping resulted in two different system designs. The storage used in Trondheim consists of 11boreholes spaced 1.5m apart. The storage volume kept the same resulting in a design of 4boreholes and a spacing of 2.5m for the system located at Siping. Where the system is build is shown to be of great importance when designing the system. Both systems reached a soil temperature above 40˚C, making them suitable for direct heating. The heating season for the two locations is mainly based on the heating load profile of the concept house. The heating season was found to be from September to March for Trondheim and from October to May for Siping.

Simulations of the solar direct heating mode show that this mode can cover 19.2% of the heating load for the system located in Trondheim and as much as 47.5% for the system in Siping. The solar radiation on is very limited during the heating season for Trondheim resulting in this low coverage. The direct heat exchange with the ground covers 27.9% of the heating load in Trondheim and manages to keep the room temperature around 21˚ C until the storage temperature goes below 35˚ C and the room temperature drops before stabilizing again. Only 11.97% of the heating load is covered by direct heat exchange with the ground for Siping. The ambient temperature reaches very low in the winter months and the room temperature drops below the set temperatures when the storage temperature goes below 36˚ C. The geothermal heat pump is covering the largest part of the heating load for the system located in Trondheim with 52.9%, while it covers 40.53% of the heating demand in Siping. The solar direct heating mode could only cover a small part for the system in Trondheim leaving a larger share for the heat pump to cover. The positive effect of a raised ground temperature was reduced since the borehole depth of the storage had to be increased for the geothermal heat pump. The initial depth of 30m resulted in freezing boreholes for both location and consequently the depth was changed to 150m for Trondheim and 200m for Siping. The COP was found to be 2.78 and 2.54 for Trondheim and Siping respectfully. For an unheated storage the COP show a small decrease ending up at 2.63 for Trondheim and 2.48 for Siping. The temperature at the inlet of the evaporator is raised since the COP is higher for a heated storage. There are not great differences since the storage depth had to be increase to avoid freezing boreholes meaning that the temperature lift left after mode 3 is not exploited.

8. Further improvement

The storage mode analyzed and investigated in this thesis is based on system optimization. The different parameters have been sized with focus on achieving high storage temperatures and a good launch pad for the heating modes. As the cost of the system is neglected the resulting design may not be economically feasible and not possible to realize. The heating load is a simple family resident whereas large borehole storages should be used for several residents to make it feasible regarding the economy versus the heating gains. Cost modeling can be achieved by utilizing the Type 588 in TRNSYS. This is an economic analysis model. However, adding an economical analysis model to the system will require a lot of research to get the right estimated for different economical parameter. The economical part is outside the scope and my theoretical expertise.

The system designed and simulated in this thesis is to some extent simplified. The ground storage should have a more accurate relationship with the real ground values at the chosen sights. The real ground consist of several layers with different compositions, groundwater and more specified for the particular location. An improvement on this area for further work is highly recommended. The ground storage model in TRNSYS is not specified enough as used in this work. The working fluid used in this system was chosen to be water, and after simulation of the heating modes the reasonable option would be an anti-freeze medium.

In reality the system would run as a single combined system. The system the combines system is divided into four separate systems simulated independently. TRNSYS is compatible with running all the four modes as one. To merge all the modes into one system required good knowledge about the software. Several valves and control systems need to be implemented to ensure correct operation time and conditions. Never the less this would result in more accurate results and it would be profitable to see how the modes interact and collaborate during operation. The exact operation time for each mode would be more precise providing more accurate results. However, the results obtained in this thesis give a good overview of the systems performance and how the system is influence by the difference in design and domestic parameters.

The heating load is also somewhat simplified and the same house design is used for both locations. For a more realistic view the house design properties should differ depending on the locations, but in this scope the parameters of the components and the system design that

was under main focus. The focus today regarding energy efficiency in buildings involve smart use of energy and “smart building”. To ensure lower energy usage there should be installed controllers/thermostats inside the different rooms of the house controlled by the occupant’s behavior. The concept house create in TRNBuild consists of one thermal zone with single zone temperature giving a simplified view if the heating load compared to the complexity of a real resident.

References

1. Yu, C., *Modeling the heating of the Green Energy Lab in Shanghai by the geothermal heat pump combined with the solar thermal energy and ground energy storage*. NTNU master thesis, 2012.
2. Geo, Q. et al., *Review of development from GSHP to UTES in China and other countries*. Elsevier B.V, 2008.
3. Kroll, J.A., & Ziegler, F., *The use of ground heat storages and evacuated tube solar collectors for meeting the annual demand in family-sized houses*. Elsevier, 2011.
4. Bauer, D., *German central solar heating plants with seasonal heat storage*. Elsevier B.V, 2009.
5. Ministry of Finance, Differensiert el-avgift for husholdniner – Energubruk i husholdningnen i Norge, NOU 2004:8.
6. Enova, *Potensial – og barrierestudie, Energieffektivisering i norske bygg,* Enovarapport 2012.
7. Berger, B et al, *Energy consumption 2012 - Household energy consumption Norway*. NVE, 2013.
8. Amecke, H et al, *Buildings Energy Efficiency in China, Germany, and the United States*. Climate politic initiative, 2013.
9. Bauer, D. (2010). German central solar heating plants with seasonal heat storage. Elsevier B.V, 2010.
10. Manghold, D., *Seasonal storage – a German success story*. Sun &Wind Energy, 2007.
11. Lundh, M.m J.O. Dalenback, *Swedish solar heated residential area with seasonal storage in rock: Initial evaluation*. Renewable Energy, 2008.
12. Chapius, S.,M. Bernier, *Seasonal storage of solar energy in borehole heat exchangers*. IBPSA Conf. Building Simulations, 2009.
13. T. KousksouP. Bruel, et al., *Energy storage: Applications and challenges*. 2013.
14. Patrice Pinel et al*., A review of available methods for seasonal storage of solar thermal energy in residential applications*. Storage concepts, 2011.
15. Sarada Kuravi et al., *Thermal energy storage technologies and systems for concentrating solar power plants***.** 2013.
16. Georgi K. Pavlov & Bjarne W.Olsen, *Seasonal ground solar thermal energy storage – review of systems and applications*.

17. European Federation of Geologists (2008). *Influence of ground conditions on geothermal installations: Guidelines to facilitate the acquisition of adequate geological data to evaluate and size GSHP projects*, GEO Trainet.
18. Florides, G., & Kalogiro, S. *Measurements of Ground Temperature at Various Depths*.
19. *Central Solar Hot Water System Design Guide.* 2011.
20. Klein, S. A. et al, *TRNSYS 16 – Manual. Madison: Solar Energy Laboratory*. University of Wisconsin-Madison, 2006.
21. Byggforskserien & Statens bygningstekniske etat, *Småhus som tilfredstiller energikravene i TEK-2007*, 2007.
22. Meteotest., *Meteonorm-Version 6.1.Bern: Meteotest*. 2009.
23. Norges geologiske undersøkelse (NGU), *Georessurser – Bergvarme,* www.ngu.no, 2008

Appendix A. Concept House

Table A1: Building description

Used area:		
UA = B · L	8 m · 16 m =	128 m^2
Area, real:		
Facade long wall	2 x 16 m x 2,5 m =	80 m^2
Facade gable wall	2 x 8 m x 2,5 m =	+ 40 m^2
Sum facade		120 m^2
Windows	9 x 1,2 m x 1,2 m=	12.96 m^2
Doors	2 x 1,0 m x 2,0 m=	+ 4.0 m^2
Sum windows and doors		16.96 m^2
Facade		120.0 m^2
Windows and doors		- 16.96 m^2
Sum wall		103,04 m^2
Areas, regulatory requirements:		
Max doors and windows	128 m^2 x 20 % =	25.6 m^2
Facade	120 m^2 – 25.6 m^2 =	94.4 m^2

Table A2: Building Shell

Wall type	Direction	Area	Windows and doors
External wall			
	North	80 m^2	9.76 m^2
	South	80 m^2	5.76 m^2
	East	40 m^2	2.88 m^2
	West	40 m^2	2.88 m^2
Floor			
	Boundary layer	128 m^2	
Ceiling			
	Boundary layer	128 m^2	
Attic			
	North (roof)	79.10 m^2	36 degrees angle
	South (roof)	79.10 m^2	36 degrees angle
	East	11.64 m^2	
	West	11.64 m^2	

Appendix B. Component Description

Table B1: TRNSYS component description

Type in TRNSYS	Description
Type 557a: Vertical U-tube ground heat exchanger	The Type 557 was developed by the Department of Physics in Lund University [10] and is the most common ground heat exchange model. It assumes uniformly placed boreholes within a cylindrical ground storage volume
Type 109: Weather data reading	Reads weather data regularly from a data file. Meteonorm provides the weather data used in this simulation.
Type 4a: Stratified water tank	The stratified tank has a volume of $10m^3$ and is fully mixed. The degree of stratification is set to N=5, where N=1 means no stratification.
Type 668: Single stage water-to-water heat pump	This model is based on user-supplied catalogue data for heating capacity and power demand, based on the entire load and source temperatures. The model interpolated date within the range of the input values specified in the data file.
Type 56: Multi-zone building	The multi-zone building can model the thermal behavior of a building with up to 25 thermal zones. In this simulation the building has one thermal zone. The building component reads information from a set of external file from TRNbuild specified by the user.
Type 735: Heating coil	The unconstrained control mode is used and the coil heats the air stream as much as possible given the inlet conditions of both the air and the fluid streams. The flow is chosen to be free floating.
Type 538: Evacuated tube solar collectors	This component used a variable speed pump keep the outlet temperature at a specified value.

Type 110: Variable speed pump	Type110 models a variable speed pump that is able to maintain any outlet mass flow rate between zero and a rated value. The controller controls the pump.
Type 111b: Variable speed fan	Type 111 models a fan that is able to turn at any speed between 0 (full stop) and its rated speed.
Type 688: Single-stage water-to-water heat pump	This model is based on user-supplied catalogue data for heating capacity and power demand, based on the entire load and source temperatures. The model interpolated date within the range of the input values specified in the data file.
Type 108: 5stage room thermostat	Type 108 is modeled to output five on/off control functions that can be used two-stage heat source, an auxiliary heater, and a two-stage cooling system. Parameters of importance are the dead band and set points. When choosing the dead bands and set points parameters one should make sure that the dead bands are not greater than the temperature difference between the set points.
Type 2b: Controller	Type 2b is an ON/OFF differential controller and controls the solar collector. The reference temperature is based on the room temperature in the building. The controller regulated the power of the circulation pump by regulating after the reference temperature.

Figure B1: Illustrations of the concept house

Appendix C. Tables and Results for storage mode Trondheim, Norway

Table C1: Numerical values for different collector area

Area	100	150	200	250	300	350
G	315621.5	315621.5	315621.5	315621.5	315621.5	315621.5
Eu	49524.45	66417.18	79729.53	90650.45	98988.16	104862
Eload	99048.9	88556.24	79729.53	72520.36	65992.11	59921.16
Etl	4289.76	6135.89	7614.57	8835.94	10862.58	14315.99
Esl	46529.16	61569.63	73553.77	83396.54	90542	94687.1
Estore	21651.23	28319.48	33557.51	37801.38	40449.55	41797.63

Table C2: Numerical values for different borehole depth

Depth	Tankloss	Eu	E_inj	E_storage_losses	E_storage
20m	10990918	91607129.2	75736283.14	35416893.77	40319389
30m	8593294	102581494	91124481.39	41735665.37	49388816
40m	7022967	110249768	101765688.6	46079792.32	55685896
50m	5903811	115852375	109518875.2	49235520.65	60283355
100m	3196816	130200743	129259353	57170335.28	72089018

Table C3: Numerical values for storage losses with different depth

Depth	E_top	E_side	E_bottom
20m	1390506	32140176.2	1886211.51
30m	989769.54	39163012.6	1582883.22
40m	724395.34	43974693.5	1380703.45
50m	536923.2	47463919.6	1234677.81
100m	72029.051	56236296.7	862009.572

Table C4: Numerical values for different borehole spacing

Spacing	E_storage	E_tankloss	Eu	E_inj	E_storageloss	T_storage
0.50	41919454.05	5098513.15	119052436.38	114672780.15	72753326.09	35.84
1.00	53315128.30	5305878.79	118274787.41	113300051.06	59984922.76	35.70
1.50	52886539.96	6625077.33	111891707.05	104167080.63	51280540.67	34.45
2.00	49388816.01	8593293.88	102581493.90	91124481.39	41735665.37	33.07
2.50	45683955.54	10408788.58	94220787.08	79477278.64	33793323.10	31.30
3.00	42149986.46	11872634.01	87646771.17	70294197.66	28144211.20	29.79
3.50	36616831.41	14143086.24	78142255.49	56865182.87	20248351.46	27.16

Table C5: Numerical values for different tank volume

Volume	T_storage	Tankloss	Eu	E_inj	E_storage_losses	E_storage
5m2	33.62	3239972.21	106446622.17	105198299.01	52280835.43	52917463.58
10m2	35.09	3960593.57	110334961.53	108072761.56	53358373.94	54714387.62
15m2	34.83	5374854.45	111234788.33	106383111.67	52451253.66	53931858.02
20m2	34.45	6625077.33	111891707.05	104167080.63	51280540.67	52886539.96
25m2	34.04	7752861.80	112547537.95	101949795.19	50114127.49	51835667.69
30m2	33.65	8785917.73	113199552.26	99834118.31	49007713.49	50826404.82

Table C6: Heat losses for a single borehole, Trondheim

	Top [MJ]	Side[MJ]	Bottom[MJ]
30m	30.46	26733.15	31.57
50m	27.85	41154.65	29.54
100m	22.31	68489.44	25.47

150m	17.93	86652.90	22.13
200m	14.64	99051.07	19.48

Appendix D. Tables and Results for storage mode Siping, China

Table D1: Energy gains and losses for varied solar collector area

	Einj	Eu	Estorage	Eloss
100m2	87166.67	83133.86	28251.56	54882.30
150m2	121035.8124	112652.988	37717.6533	74935.33
200m2	149324.7375	137141.296	45225.8164	91915.48
250m2	170720.69	154484.866	49530.7228	104954.1
300m2	186948.3622	165600.635	51757.7031	113842.9
350m2	201551.6474	173292.039	53565.8891	119726.2

Table D2: Energy gains and losses for varied storage depths

Depth [m]	Tankloss	Eu	E_inj	E_storage_losses	E_storage
10m	5057651.662	56503161.83	49106445.47	26298978.84	22807466.64
20m	2929694.071	71644569.13	68265485.63	33592529.8	34672955.82
30m	1874087.426	79924307.92	78890537.1	37944454.91	40946082.18
40m	1230069.635	85108895.75	85630047.6	40663885.78	44966161.82
50m	802643.5741	88880938.33	90516873.04	42649104.17	47867768.87
100m	-138913.273	97791321.56	101996614.4	47224252.75	54772361.62

Table D3: Storage losses for different borehole depth

Depth [m]	E_top	E_side	E_bottom
10m	1723032.651	22037533.14	2538413.045
20m	850251.3277	30835844.7	1906433.78
30m	392877.4257	35997360.73	1554216.758
40m	110919.2535	39221703.51	1331263.018
50m	-77790.31212	41547972.41	1178922.073
100m	-502331.3597	46922006.83	804577.2826

Table D4: Numerical values for different borehole spacing

Spacing	T_storage	Tankloss	Eu	E_inj	E_storage_losses	E_storage
0.5m	31.57588959	6741186.342	45937361.95	35714502.9	12702156.39	23012346.5
1m	34.88119888	5567921.569	52955315.55	44599672.93	17940997.93	26658675
1.5m	37.05054855	4780955.069	57976020.31	50963129.34	21827653.14	29135476.21
2m	39.6810112	3833555.743	64774344.86	59484063.84	27505843.82	31978220.02
2.5m	42.01741409	2929694.071	71644569.13	68265485.63	33592529.8	34672955.82
3m	44.47922134	2057765.346	78334767.03	77558559.9	41549094.74	36009465.16
3.5m	45.93087387	1897891.516	79538725.77	79965593.54	51307797.39	28657796.15

Appendix E. Tables and Results the storage mode

Table E1: Absolute amount of energy gains and energy losses in storage mode

Outputs [MJ]	Trondheim	Siping
G	330591.5	461359.9
E_u	109957.2	131163.9
E_{load}	105496.9	117820.2
E_{sl}	67112.2	78888.1
E_{store}	32437.5	41724.9
E_{inj}	88887.3	120612.9

Appendix F. Tables and Results the heating modes

G.1. Mode 2: Solar direct heating mode

Table F1: Numerical values for simulation of mode 2, Trondheim

Month	Coil	Rad	House	SF
Sept	0.00	330.53	861.82	0.00
Oct	1567.43	180.66	4991.93	0.31
Nov	3222.83	80.44	9219.16	0.35
Des	1449.27	36.50	12094.97	0.12
Jan	1536.73	64.11	11256.61	0.14
Feb	4662.61	183.15	10252.6	0.45
Mar	4380.17	361.96	7031.61	0.62
Apr	782.87	504.10	3439.46	0.23
May	0.00	602.51	1143.92	0.00

Table F2: Numerical values for simulation of mode 2, Siping

Month	Coil	Rad	House	SF
Oct	472.64	504.76	2249.12	0.21
Nov	4225.12	405.99	9714.19	0.43
Des	8805.99	377.88	17186.33	0.51
Jan	10956.42	400.28	19952.85	0.55
Feb	7838.62	488.79	15783.08	0.50
Mar	3070.67	593.09	7917.6	0.39
Apr	403.72	569.25	1886.66	0.21

Appendix G. Calculations

G.2. Calculations of Building heat load

Trondheim

Annual heating demand = 44553968.23kJ/hr = 44553968.23/hr /3600 =12376.1KW

House Area = 128m^2

Annual heating demand =12376.1KW/128m^2 = 98.69KW/m^2

Siping

Annual heating demand = 54222310.15/hr = 54222310.15hr /3600 =15061.75KW

House Area = 128m^2

Annual heating demand = 15061.75KW/128m^2 = 117.67KW/m^2

G.3. Ratios and efficiencies

Table G1: Efficiencies and rates

Results	Borehole depth [m]				
	20	30	40	50	100
F_{StU}	47.93	53.43	56.66	58.79	63.48
F_{StL}	64.81	65.80	66.33	66.66	67.42
F_F	11.16/11.99	7.86/8.38	6.01/6.37	4.84/5.09	2.40/2.46
F_{LU}	32.29	33.94	34.84	35.40	36.51
24hr					
Tank efficiency	36.34	32.34	29.25	26.81	20.38
Thermal efficiency	34.64	35.03	35.28	35.55	36.26
Efficiency	11.36	12.36	13.67	14.37	17.28

$$F_{StU} = \frac{E_{store}}{E_u}$$

Equation G1: Ratio of stored energy to useful solar energy gain

$$F_{StL} = \frac{E_{store}}{E_{load}}$$

Equation G2: Ratio of stored energy to energy injected

$$F_T = \frac{E_{tl}}{E_{load}}$$

Equation G3: Ratio of tank losses to useful solar energy gain

$$F_{LU} = \frac{E_{sl}}{E_u} = 100\% - F_{SU} - F_T$$

Equation G4: Ratio of storage losses to useful solar energy gain

$$F_{LL} = \frac{E_{sl}}{E_{load}} = 100\% - F_{SL}$$

Equation G5: Ratio of storage losses to injected energy

G.4. Calculations of the efficiencies in the solar collector, Trondheim

$$\eta_{sys} = \frac{E_u}{I \times A}$$

Equation G6: Solar collector efficiency

$$\eta_{100m^2} = \frac{38720972}{101529429} = 38.14$$

$$\eta_{150m^2} = \frac{55706959.4}{152294143.5} = 36.58$$

$$\eta_{200m^2} = \frac{71136780}{203058858} = 35.03$$

$$\eta_{250m^2} = \frac{85248081}{253823572} = 33.58$$

$$\eta_{300m^2} = \frac{97952138}{304588287} = 32.16$$

$$\eta_{350m^2} = \frac{109709403}{355353001} = 32.16$$

G.5. Calculations of the COP, Trondheim

$$COP_{24\,hr} = \frac{\int_0^{24} Q_{storage}\,dt}{(El_{sc} + El_{BTES}) \times t}$$

Equation G7: COP over 24 hours

For the 1.July

$$COP_{24\,hr} = \frac{51596.63MJ \times 24h}{(1223.9 + 2415.6)MJ \times 13h} = 26.17$$

Period

Jun – Aug

$$COP = \frac{54714387.62 \times 2208}{(2691786.28 + 6687862.37) \times 803} = 16.04$$

Jun – Sep

$$COP = \frac{77979443.84 \times 2928}{(4446102.36 + 11697816.77) \times 970} = 14.58$$

Mai – Aug

$$COP = \frac{81268996.23 \times 2954}{(4529462.04 + 11936333.11) \times 1031} = 14.14$$

Mai - Sep

$$COP = \frac{106520135.73 \times 3672}{(6716956.93 + 18395647.51) \times 962} = 16.19$$

G.6. Calculations of heat per tube length

$$Heat\ per\ tube\ length = \frac{Heat\ stored[MJ]}{tube\ length\ [m]}$$

$$Trondheim = \frac{32437.5}{(11\times30m)} = 147.44\frac{MJ}{m^2}$$

$$Siping = \frac{41724.9}{(4\times30m)} = 347.7\frac{MJ}{m^2}$$

G.7. Calculations of the new storage parameters for heating mode 4.

$$Q_{load} = \rho c_p V\left(T_{fin} - T_{fout}\right)$$

Equation G8: Heat load, heating mode 4

$$T_a = \frac{V_1 T_{30} + V_2 T_g}{V_1 + V_2}$$

Equation G8: New estimated ground temperature

Calculations for Trondheim:

$V_1 = 623.45\text{m}^3$

$T_{30} = 30^\circ\text{C}$

$V_2 = 3214.66\text{m}^3$

$T_g = 7.7^\circ\text{C}$

$T_a = 10.81^\circ\text{C}$

Calculations for Siping:

$V_1 = 623.45\text{m}^3$

$T_{30} = 30^\circ\text{C}$

$V_2 = 4329.51\ \text{m}^3$

$T_g = 9.17^\circ\text{C}$

$T_a = 11.79^\circ\text{C}$